Office of Naval Research
Department of the Navy
Contract Nonr 220(35)

A WAKE MODEL FOR FREE-STREAMLINE FLOW THEORY PART II. CAVITY FLOWS PAST OBSTACLES OF ARBITRARY PROFILE

by

T. Yao-tsu Wu and D. P. Wang

Hydrodynamics Laboratory
Kármán Laboratory of Fluid Mechanics and Jet Propulsion
California Institute of Technology
Pasadena, California

Report No. 97-4

May, 1963

A WAKE MODEL FOR FREE-STREAMLINE FLOW THEORY PART II. CAVITY FLOWS PAST OBSTACLES OF ARBITRARY PROFILE

by

T. Yao-tsu Wu and D. P. Wang

Kármán Laboratory, California Institute of Technology

In Part I of this paper a free-streamline wake model was introduced to treat the fully and partially developed wake flow or cavity flow past an oblique flat plate. This theory is generalized here to investigate the cavity flow past an obstacle of arbitrary profile at an arbitrary cavitation number. Consideration is first given to the cavity flow past a polygonal obstacle whose wetted sides may be concave towards the flow and may also possess some gentle convex corners. The general case of curved walls is then obtained by a limiting process. The analysis in this general case leads to a set of two functional equations for which several methods of solution are developed and discussed.

As a few typical examples the analysis is carried out in detail for the specific cases of wedges, two-step wedges, flapped hydrofoils, and inclined circular arc plate. For these cases the present theory is found in good agreement with the experimental results available.

---

1. Introduction

The general theory of potential flows past curved obstacles with a free boundary formation has been long recognized as an interesting but difficult mathematical problem. The questions of construction, calculation, as well as existence and uniqueness have intrigued many outstanding hydrodynamicists and mathematicians alike. The celebrated work of Levi-Civita (1907) for the infinite cavity case has provided the basis for the general theory by introducing a convenient parametrization of the

flow by which the solution is expressed in terms of an arbitrary analytic function in a half unit circle, and thereby removing the unknown free boundary from the question. Levi-Civita's representation has been further advanced by Villat (1911) who formulated the flow problem in terms of functional integral equations which have played a central role in the existence theory and the actual construction of the solution. Detailed discussions of these fundamental articles and the related developments can be found in the recent literature on this subject, for example, see Gilbarg (1960), Birkhoff and Zarantonello (1957).

It has been noticed that perhaps the most complex and difficult problem of all is the actual computation of the solution. Some practical aspects of these difficulties have been discussed by Birkhoff and Zarantonello (Chapter 9). This problem is somewhat unavoidable since for cavity flows past curved obstacles, even with infinite cavities, the numerical methods seem to be the only means of obtaining an accurate solution from the exact theory. While several finite-cavity flow models have also been considered together with the corresponding functional equations of Villat's type (see, e.g., Gilbarg, 1960), the incorporation of these models only magnifies the complexities of the computation. One approximate method in common use is to discretize the continuous curvature equation by a polynomial representation and to solve the resulting set of equations by direct iteration. However, this iteration has been shown to diverge for large values of a certain parameter M (which relates the scale of potential and that of the physical plane); for such cases a more eleborate averaged iteration has been introduced by Birkhoff, Goldstine and Zarantonello (1954). From our experience, the difficulties becomes particularly noticeable in the case of thin curved barriers held at small incidences to the flow since the total variation of the integrand in the functional equations increases rapidly with decreasing angle of attack. Unfortunately, this is also the case of considerable interest from the viewpoint of practical applications, such as the cavitating hydrofoils and stalled airfoils. In short, it seems that so far none of the general iteration methods have been rigorously proved to converge, and theoretical estimates of error are still lacking.

The main objectives of this paper are two-fold: (1) first to develop an exact theory for the general case of arbitrary body profile and arbitrary cavitation number by adopting a rather simple wake model and by using a different parametrization, (2) to examine various numerical schemes which can be applied uniformly in the incidence angle and the cavitation number.

In Part I of this paper (Wu, 1962) a free-streamline wake model was introduced to treat the flow past an oblique flat plate with a fully or partially developed wake (or cavity) formation. According to this model the wake flow is approximately described in the large by an equivalent potential flow past the body with an infinitely long wake which consists of a near-wake of constant under-pressure and a far-wake trailing downstream. The pressure increases continuously back to its free stream value along the far-wake boundary which is assumed to form a branch slit of an unknown shape in the hodograph plane.

This theory will now be generalized to evaluate the wake (or cavity) flow past an obstacle of arbitrary profile at arbitrary cavitation number. Consideration is first given to a polygonal obstacle whose wetted sides may be concave towards the flow and may also possess some gentle convex corners. The parametric plane of the flow is chosen to be in a half unit circle, with the circular arc corresponding to the constant pressure free boundary and the diameter to the wetted surface in such a way that this plane becomes the hodograph as the polygon is degenerated to a flat plate. The general case of curved walls is then deduced by a limiting process. The analysis in this general case leads to a set of two functional equations which are quite similar to Villat's equations. These equations immediately provides the exact solution of a wide class of the "inverse problems". While the general direct problems are still difficult to solve exactly, the computation of the present theory is however not further complicated by non-vanishing cavitation numbers (aside from the determination of an additional scalar parameter). Several numerical methods for the general purpose have been developed here, some of which have already been applied with success.

In order to exhibit some salient features of cavity flows past curved obstacles, such as the effects of camber, cavitation number, incidence angle, and so forth, as well as to achieve a sound grasp of the convergence of various numerical schemes, the analysis and the subsequent computation have been carried out in detail for several typical examples: wedge, two-step wedge, hydrofoil with a flap, and inclined circular arc plate. The adopted methods have been found to converge in every case tried. Furthermore, in these cases the present theory is found in good agreement with the experimental results available.

2. Cavity Flows and Wake Flows Past a Polygonal Obstacle; Parametrization

We consider first the steady, plane, potential flow of an incompressible fluid past a polygonal obstacle with a wake or cavity formation in such a way that the N sides of the polygon are wetted and the flow is separated from fixed leading and trailing edges A and B, forming two free streamlines ACI and BC'I, as shown in the physical plane $z = x + iy$ of Figure 1. The free stream at infinity is inclined at an angle α with the x-axis which may be chosen (but not necessarily) to coincide with the chord AB. Let $z_o = z_A, z_1, z_2, \ldots, z_N = z_B$ be the vertices of the polygon; and let $(1 + \epsilon_k)\pi$ be the exterior angle (on the cavity side) subtended by the consecutive sides at z_k, $k = 1, 2, \ldots (N-1)$.

The polygonal wall may be concave towards the flow and may also possess some gentle convex corners so long as the resulting flow configuration provides a valid approximation of the actual physical flow. It is noted that the potential flow at such a convex corner, if not a stagnation point, must be singular there. Whether the flow is actually separated or not from such convex corners, however, should be investigated by including the relevant real fluid effects such as the viscous boundary layer at the wall, convection and diffusion of dissolved gases, as well as other properties of incipient cavitation These real fluid effects are rather complicated and difficult to be taken into an accurate account; they will not be further discussed in this work. In the present formulation the flow around such convex corners may be regarded as an approximation to the actual

case in which either the real fluid effects under the circumstances keep the flow from being separated or there exists only a small separated bubble with an immediate reattachment to the solid surface, so that no serious error is resulted from neglecting such detailed local structure of the flow. To permit such gentle convex corners to remain wetted in the cavity flow is very essential when we later generalize this analysis by a limiting process for obstacles of arbitrary profile. With this additional degree of freedom, ϵ_k is positive or negative according as the boundary at z_k is concave or convex towards the flow. It should be emphasized, nevertheless, that due caution must be exercised to consider the possibility of change in the basic flow pattern (such as the flow in Figure 1 may change the separation point from B to z_3 for small enough α, thus leaving z_3B inside the cavity).

Adopting the same notation as in Part I, we have the complex potential $f(z) = \varphi + i\psi$, and the complex velocity

$$w(z) = df/dz = u - iv = q e^{-i\theta}. \tag{1}$$

The free stream has velocity U and incidence angle α, so

$$w = U e^{-i\alpha} \qquad at \qquad z = \infty. \tag{2}$$

The general description of the present wake flow model has been given in Part I, which may be summarized here for the convenience of subsequent application. The part AC and BC' of the free streamlines form the lateral boundary of a near-wake of constant pressure

$$p = p_c < p_\infty \qquad on \quad AC \quad and \quad BC', \tag{3}$$

p_∞ being the free stream pressure. From this part onward p varies continually and monotonically from p_c to p_∞ along the far-wake boundary, CI and C'I. It is further assumed that

$$f_C = f_{C'}, \qquad w_C = w_{C'}. \tag{4}$$

Moreover, the images of the free streamlines CI and C'I are assumed to form a branch slit of undetermined shape in the w-plane (the hodograph-slit condition). The Bernoulli equation of the external flow is

$$p + \tfrac{1}{2}\rho q^2 = p_\infty + \tfrac{1}{2}\rho U^2 = p_c + \tfrac{1}{2}\rho q_c^2 , \tag{5}$$

where q_c is the constant value of q along AC and BC'. With q_c normalized to unity, we have

$$q_c = 1, \qquad U = (1+\sigma)^{-1/2}, \tag{6a}$$

where

$$\sigma = (p_\infty - p_c)/(\tfrac{1}{2}\rho U^2), \tag{6b}$$

σ being the wake under-pressure coefficient, or the cavitation number for cavity flows. Condition (3) is written for the case of full wake flow; for the partial wake flow case (see Part I for further details) the constant pressure portion BC' behind the trailing edge B then disappears.

For the present problem we introduce the ζ and t parameter planes by

$$f = \tfrac{1}{4} A (\zeta - \zeta_o)^{-1} (\zeta - \bar{\zeta}_o)^{-1}, \tag{7}$$

$$\zeta = \tfrac{1}{2}(t + t^{-1}), \tag{8}$$

where A is a real positive constant and the complex constant ζ_o is the image point (yet undetermined) of $z = \infty$. The flow regions in the ζ and t-plane are shown in Figure 1. The local conformal behavior at C and C' requires that $df/d\zeta = O(|\zeta - \zeta_C|)$ as $|\zeta - \zeta_C| \to 0$, from which it follows

$$\zeta_C = \zeta_{C'} = \mathrm{Re}\ \zeta_o . \tag{9a}$$

Moreover, the line segments CI, C'I and DI are seen from (7) to be straight lines parallel to the Im ζ-axis. The fully cavitating flow is again specified by the condition that the point C' falls downstream of the trailing edge B, or

$$\zeta_{C'} = \mathrm{Re}\ \zeta_o \leq 1 . \tag{9b}$$

When the numerical result gives Re $\zeta_o > 1$ the flow may be supposed to have undergone transition to become partially cavitating.

Equations (7) and (8) can be combined to give

$$f(t) = A t^2 \left[(t - t_o)(t - \bar{t}_o)(t - t_o^{-1})(t - \bar{t}_o^{-1}) \right]^{-1} \tag{10}$$

where t_o, from (8), is given by $t_o = \zeta_o - (\zeta_o^2 - 1)^{\frac{1}{2}}$. The use of the variable t is suggested by the analysis of Part I: here t plays the role of the variable w of the wake flow past an oblique flat plate (see Part I) so that with $t \equiv w$, (10) provides the required solution of the flat plate problem.

The solution of the present problem is seen to be best represented in the parametric form f = f(t) and w = w(t). We proceed now to determine the latter part w = w(t). Let the points $\tau_1, \tau_2, \ldots \tau_{N-1}$ on the real diameter of the t-plane ($-1 < \tau_1 < \tau_2 < \ldots < \tau_{N-1} < 1$) correspond to the vertices $z_1, z_2, \ldots z_{N-1}$ of the wall. We further let the stagnation point D, at which w = 0, be chosen at t = 0. Now, as the point z moves along the polygonal boundary from A to B, Im (log w) = arg w remains constant on every straight segment, jumps by $(\epsilon_k \pi)$ as z moves across the vertex z_k, and jumps by π as z goes over the stagnation point. Furthermore, along AC and BC', where $|t| = 1$, we have Re(log w) = log q_c = 0. From these two conditions one sees by inspection that

$$w(t) = e^{-i\beta_o} t \prod_{k=1}^{N-1} \left(\frac{t - \tau_k}{\tau_k t - 1} \right)^{\epsilon_k} \tag{11}$$

where β_o is the angle made by the leading segment with the x-axis, positive in the counterclockwise sense. It is obvious that the above w satisfies the conditions on arg w over the solid boundary. Furthermore, with $-1 < \tau < 1$ and δ real, the conformal transformation

$$T = \exp(i\delta)\,(t - \tau)/(\tau t - 1) \tag{11a}$$

maps the circle $|t| = 1$ on $|T| = 1$, and we have $|T| < 1$ when $|t| < 1$. This establishes the solution (11). In particular, when β_o and all ϵ_k

vanish, w and t become identical, leaving (10) as the known solution of the flat plate problem (see Part I).

Equations (10) and (11) give the parametric solution f = f(t), w = w(t). The solution is completed when the physical z-plane is determined from

$$z(t) = \int_{-1}^{t} \frac{1}{w(t)} \frac{df}{dt}\, dt . \tag{12}$$

The above integral in general cannot be integrated in a closed form.

It is noted that the solution given by (10), (11) and (12) contains (N + 1) parameters A, t_o, τ_1, ... τ_{N-1} (N + 2 real parameters as only t_o is complex) which can be determined by the following consideration. First, at $z = \infty$, or $t = t_o$, application of condition (2) to (11) yields

$$U e^{i(\beta_o - \alpha)} = t_o \prod_{k=1}^{N-1} \left(\frac{t_o - \tau_k}{\tau_k t_o - 1} \right)^{\epsilon_k} . \tag{13}$$

The region of $|t_o|$ for the particular case of all $\epsilon_k > 0$ can be seen from (13), (11a) to be:

$$U < |t_o| < 1, \qquad \text{if all } \epsilon_k > 0. \tag{13a}$$

Furthermore, the length of the kth segment is

$$\ell_k \equiv |z_k - z_{k-1}| = \int_{\tau_{k-1}}^{\tau_k} \frac{1}{|w|} \left| \frac{df}{dt} \right| dt , \qquad k = 1, 2, \cdots N. \tag{14}$$

Finally, we also have

$$z_B - z_A = \int_{-1}^{1} \frac{1}{w} \frac{df}{dt}\, dt = \ell\, e^{i\alpha_c} \tag{15}$$

Where ℓ is the chord length and α_c the inclination of the chord. Equations (13) and (14) are (N + 1) equations, which are in general nonlinear and transcendental, for the (N + 1) parameters A, t_o, τ_1, ... τ_{N-1}. For further discussion on the determination of these parameters, we distinguish between the following two cases.

3. The Direct and Inverse Problem; Numerical Iteration Methods

The original physical or direct problem is specified with prescribed geometry (given all ℓ_k and ϵ_k) and the flow configuration (given α and the cavitation number σ (or U)), in total there being (2N + 1) direct physical parameters

$$P(\alpha;\ \sigma;\ \ell_1, \cdots \ell_N\ ;\ \epsilon_1, \cdots \epsilon_{N-1}). \tag{16a}$$

A wake flow past a N-sided polygon can therefore be represented by a point P in a (2N + 1)-dimensional space with the above coordinates. The region of these coordinates permissible for our physical problem may be described as

$$R\ (\ |\alpha| < \tfrac{\pi}{2}\ ;\ \sigma > 0;\ \ell_k > 0\ ;\ \delta_k < \epsilon_k < 1\ ) \tag{16b}$$

where δ_k, the lower limit of ϵ_k, may be zero or may assume some small negative value (in order to render a valid approximation of the actual motion, as explained earlier). Aside from this qualifying condition, no definite lower bound of the negative value can be stated in general for δ_k. If, however, $\delta_k \geq 0$, k = 1, 2 ... N-1, then the wetted surface is concave to the flow.

On the other hand, our solution given by (10)—(14) also defines a wake flow past a N-sided polygon which can be represented by (2N + 1) "inverse flow" parameters

$$P'(A;\ t_0(\text{complex});\ \tau_1, \cdots \tau_{N-1}\ ;\ \epsilon_1, \cdots \epsilon_{N-1}) \tag{17a}$$

with the corresponding region

$$R'(A>0;\ |t_0|<1,\ -\pi < \arg t_0 < 0\ ;\ -1 < \tau_1 < \cdots < \tau_{N-1} < 1;\ \delta_k < \epsilon_k < 1). \tag{17b}$$

For the more restricted case of $\delta_k = 0$ in (16b) and (17b) the corresponding region will be denoted by R_* and R_*'. For definiteness some statement in the sequel will be made on the basis of the region R_* and R_*' since the relaxed case when ϵ_k may assume small negative values must

eventually depend on experimental verification.

Let us consider the inverse problem by choosing a point P' within the region $R_{\mp}'$. Then, since $|\tau_k| < 1$ and $|t_o| < 1$, it follows from (13) that

$$U = |t_o| \prod_{k=1}^{N-1} \left| \frac{t_o - \tau_k}{\tau_k t_o - 1} \right|^{\epsilon_k} < 1 \qquad (18a)$$

so that $\sigma = (U^{-2} - 1) > 0$. Equating the argument of (13), we obtain the incidence $(\alpha - \beta_o)$ of the leading segment

$$\alpha - \beta_o = - \arg t_o + \sum_{k=1}^{N-1} \epsilon_k \left[\arg (\tau_k t_o - 1) - \arg (t_o - \tau_k) \right]. \qquad (18b)$$

The entire configuration is then fixed (up to a common scale factor A), with the length ℓ_k of every segment given by (14). Therefore, to each P' in R_{*}' there corresponds a single P in $R_{\mp}$. In this sense we may assert that the mathematical solution of an inverse problem <u>exists</u> and is <u>unique</u>.

In the direct problem with prescribed P, there are (N + 1) unknown parameters A; t_o; $\tau_1, \ldots \tau_{N-1}$, which have to be determined from the (N + 1) transcendental equations (13) and (14). These equations are in general very difficult to solve directly. The existence and uniqueness consideration for the original physical problem is to establish the converse statement that to each point P there corresponds one and only one P', or in other words that the (N + 1) nonlinear equations (13) and (14) possess a unique solution of the (N + 1) unknown parameters for any perscribed values of the physical parameters in P. The problem of existence and uniqueness may be treated by adopting the idea of "local uniqueness" as used by Weinstein (1924, 1927, 1929), and Leray (1934, 1935) for similar problems in the theory of free boundary flows. The details of such considerations, however, will not be pursued further in this work.

The above consideration of the inverse problem provides a basis of constructing approximate methods for the direct physical problem.

We have essentially established two such methods: (i) an integral iteration scheme and (ii) a differential perturbation approximation, both depending on a known basic flow as the reference. The difference between the actual flow and the basic flow need not be very small for the first method as long as the iteration converges, whereas this difference is assumed small for the second method to be effective. The integral iteration for polygonal obstacles is best presented as a special case of the general method for curved profiles; this is done in Section (5A). We present below the differential perturbation method as it may also bear some interest regarding the problem of existence and uniqueness.

Suppose that a basic flow $P(\alpha;\ \sigma;\ \ell_1, \cdots \ell_N;\ \epsilon_1, \cdots \epsilon_{N-1})$ is given by (13) and (14) with prescribed parameters $P'(A;\ t_o;\ \tau_1, \cdots \tau_{N-1};\ \epsilon_1, \cdots \epsilon_{N-1})$. Let these parameters be given variations δA, δV, $\delta \alpha_o$, $\delta \tau_k$, $\delta \epsilon_k$, where $t_o = V e^{-i\alpha_o}$. Then the corresponding variation of the physical parameters is given by

$$\delta \ell_j = \frac{\partial \ell_j}{\partial A}\delta A + \frac{\partial \ell_j}{\partial V}\delta V + \frac{\partial \ell_j}{\partial \alpha_o}\delta \alpha_o + \sum_{k=1}^{N-1}\left(\frac{\partial \ell_j}{\partial \tau_k}\delta \tau_k + \frac{\partial \ell_j}{\partial \epsilon_k}\delta \epsilon_k\right), \tag{19a}$$

$$\delta \epsilon_k = \delta \epsilon_k \qquad (k = 1, 2, \cdots N-1), \tag{19b}$$

$$\delta U = \frac{\partial U}{\partial V}\delta V + \frac{\partial U}{\partial \alpha_o}\delta \alpha_o + \sum_{k=1}^{N-1}\left(\frac{\partial U}{\partial \tau_k}\delta \tau_k + \frac{\partial U}{\partial \epsilon_k}\delta \epsilon_k\right), \tag{19c}$$

$$\delta \alpha = \frac{\partial \alpha}{\partial V}\delta V + \frac{\partial \alpha}{\partial \alpha_o}\delta \alpha_o + \sum_{k=1}^{N-1}\left(\frac{\partial \alpha}{\partial \tau_k}\delta \tau_k + \frac{\partial \alpha}{\partial \epsilon_k}\delta \epsilon_k\right), \tag{19d}$$

where in (19a), $j = 1, 2, \ldots N$. In (19c) U may be replaced by σ since $\sigma = (U^{-2} - 1)$. The coefficients of the above set of $(2N + 1)$ equations can be readily deduced by differentiations of (13) and (14); their explicit expressions hence will not be given here.

Conversely, if a physical flow is given by $P_*(\alpha;\ \sigma;\ \ell_k + \delta \ell_k;\ \epsilon_k + \delta \epsilon_k)$ which in turn may be regarded as a variation of the basic flow at fixed α and σ, then the corresponding variation of the inverse parameters can be obtained by solving the $(2N + 1)$ linear equations (19)

with the known quantities $\delta \ell_k$, $\delta \epsilon_k$, $\delta U = 0$, $\delta \alpha = 0$, provided that the Jacobian

$$\partial(\alpha; \sigma; \ell_1, \cdots \ell_N; \epsilon_1, \cdots \epsilon_{N-1}) / \partial(A; V; \alpha_o; \tau_1, \cdots \tau_{N-1}; \epsilon_1, \cdots \epsilon_{N-1}) \tag{20}$$

is nonvanishing. The last statement would also imply existence and uniqueness.

The above perturbation theory can be applied to construct an iteration scheme as follows. We combine the so determined variation (δA, δV, δa_o, $\delta \tau_k$, $\delta \epsilon_k$) with the original reference flow to provide a new reference flow P_1' ($A + \delta A$, $V + \delta V$, $a_o + \delta a_o$, $\tau_k + \delta \tau_k$, $\epsilon_k + \delta \epsilon_k$) which, by using (13) and (14) as an inverse problem, provides in turn a new physical flow P_1 ($a^{(1)}$, $\sigma^{(1)}$, $\ell_k^{(1)}$, $\epsilon_k^{(1)}$). By comparison of P_1 with the given flow P_* a set of new variation (δa, $\delta \sigma$, $\delta \ell_k$, $\delta \epsilon_k$) of the physical parameters is obtained, thus enabling one to proceed by repeating the process iteratively over and over again. Needless to say, the success of this iteration process depends on how fast the set P_n ($a^{(n)}$, $\sigma^{(n)}$, $\ell_k^{(n)}$, $\epsilon_k^{(n)}$) converges to the prescribed physical flow.

It may be remarked that the first reference flow need not have the same number of N faces. For example, when all the ϵ_k's are small, the cavity flow past the flat plate spanning along the chord AB can be used as the basic flow, in which case the complex velocity w of the basic flow coincides with t, and $\tau_1, \cdots \tau_{N-1}$ of the basic flow become the image in the t-plane of those points on the flat plate which are at the same length apart as the vertices of the given polygon (in other words, $\delta \ell_k$ are all chosen to be zero for the first iteration).

4. Obstacles with Arbitrary Profile; The Functional Equations

The preceding results can be readily extended to contain the general case when the obstacle has an arbitrary profile. This generalization is quite straightforward for the case of fixed detachment when the detachment points (in general at sharp corners) are assumed known. The theory can also be applied to the problem of smooth detachment,

when the detachment points (at a smooth surface, for example) cannot be prescribed in advance, provided some additional appropriate conditions are imposed for their determination. The condition generally adopted for this type of problem is based on Villat's criterion (1914) which requires the curvature of the free streamline to be finite at the point of smooth detachment.

Thus we presume that the free streamlines become detached from the body at points A and B (with either fixed or smooth detachment) to form a wake or cavity, as depicted in Figure 2. The wetted surface of the obstacle may be expressed parametrically as

$$x = x(s), \quad y = y(s), \qquad \text{for} \quad 0 \leqslant s \leqslant S, \tag{21a}$$

where S is the total arc length of the wetted surface. These functions and their first derivatives may be assumed Hölder continuous in s for $0 \leqslant s \leqslant S$. The inclination angle of the body surface with the x-axis is

$$\beta(s) = \arctan\left(\frac{dy}{ds} \Big/ \frac{dx}{ds}\right), \qquad 0 \leqslant s \leqslant S. \tag{21b}$$

Here the variation of β need not be limited small as long as the resulting flow is supported by physical observations. The maximum variation of β, defined as the difference between the maximum and minimum value of β, may be taken to be less than π and may be considerably smaller in ordinary cases of practical applications.

Let us consider a limiting process by which the number N of the polygonal faces increases beyond all bounds, the face lengths ℓ_k all tend to zero, and the turning angles ϵ_k all become vanishingly small except possibly at a finite number of isolated points where the obstacle has sharp corners. In the limit as $N \to \infty$ and $|\epsilon_k| \to 0$, we may rewrite (11) as

$$w = e^{-i\beta_0}\, t \exp\left\{ \sum_{k=1}^{N-1} \epsilon_k \log\left(\frac{t-\tau_k}{\tau_k t - 1}\right)\right\},$$

and then replace the summation by an integration with respect to the continuous variable τ, substituting $\epsilon_k \pi$ by $(-d\beta)$ where $\beta(\tau)$ is the inclina-

tion angle of the body surface at the point $t = \tau$. (The negative sign of $(-d\beta)$ is taken on account of the original convention of the positive sense of ϵ_k.) We therefore obtain

$$w = e^{-i\beta_o}\, t\, \exp\left\{-\frac{1}{\pi}\int_{-1}^{1} \log\left(\frac{t-\tau}{\tau t-1}\right)\frac{d\beta}{d\tau}\,d\tau\right\} \tag{22}$$

where clearly $\beta_o = \beta(-1)$. It may be noted that this result includes the special case (11) for the polygonal bodies when we take

$$\frac{d\beta}{d\tau} = -\sum_{k=1}^{N-1} (\epsilon_k \pi)\,\delta(\tau-\tau_k),$$

$\delta(\tau - \tau_k)$ being the Dirac delta function. Integrating the integral in (22) by parts, we find that the contribution at the lower limit $\tau = -1$ (where $\beta = \beta_o$ and $\log[(t-\tau)/(t\tau-1)] = i\pi$) cancels the factor $\exp(-i\beta_o)$, giving

$$w(t) = t\,\exp\left\{-\frac{(1-t^2)}{\pi}\int_{-1}^{1}\frac{\beta(\tau)\,d\tau}{(\tau-t)(\tau t-1)}\right\}. \tag{23}$$

The exact solution is therefore expressed parametrically as $f = f(t)$, $w = w(t)$, with $f(t)$ given by (10) and $w(t)$ by (22) or (23). As a remark, the above solution $w(t)$ can also be obtained directly by the method of functional theory (see Appendix).

The form (22) is based on the curvature whereas (23), on the inclination of the body surface. In fact, the curvature of a bounding streamline, defined by $\kappa = d\theta/ds$ (s being the arc length along the streamline), can be written

$$\kappa = \frac{d\theta}{ds} = \frac{\partial\theta}{\partial\varphi}\frac{\partial\varphi}{\partial s} = Re\left(q\,\frac{d\omega}{df}\right) = Re\left(e^{\lambda}\,\frac{d\omega}{df}\right), \tag{24a}$$

where

$$\omega = i\log w = \theta + i\lambda. \tag{24b}$$

Hence on the body, $\theta = \beta$ (or they may differ by at most a constant),

$$\kappa_S = q\,\frac{d\beta}{d\varphi} = e^{\lambda(t)}\,\frac{d\beta}{dt}\Big/\frac{df}{dt}, \qquad -1 < t < 1\ ; \tag{25a}$$

and on the cavity boundary where $\lambda = 0$,

$$\kappa_c = \frac{d\omega}{df} = \frac{d\omega}{dt} \Big/ \frac{df}{dt}, \qquad t = e^{-i\chi}, \quad 0 < \chi < \pi. \tag{25b}$$

Finally, the physical z-plane is again determined by (12), except now w(t) is given by (22) or (23). In particular, on the body (t real),

$$z(t) = \int_{-1}^{t} e^{i\beta(t)} \exp\left\{ \frac{(1-t^2)}{\pi} \int_{-1}^{*1} \frac{\beta(\tau)\, d\tau}{(\tau - t)(\tau t - 1)} \right\} \frac{df}{dt} \frac{dt}{t}, \tag{26a}$$

in which $*$ above the integral sign signifies the Cauchy principal value. Since for real t,

$$\int_{-1}^{*1} \frac{d\tau}{(\tau - t)(\tau t - 1)} = 0,$$

we may also write for the points on the solid surface, or for t real,

$$z(t) = \int_{-1}^{t} e^{i\beta(t)} \exp\left\{ \frac{(1-t^2)}{\pi} \int_{-1}^{1} \frac{\beta(\tau) - \beta(t)}{(\tau - t)(\tau t - 1)} d\tau \right\} \frac{df}{dt} \frac{dt}{t}. \tag{26b}$$

Since $dz = (ds) e^{i\beta}$, it therefore follows from (26b) that the arc length s(t) along the body surface, measured from the leading edge A, is

$$s(t) = \int_{-1}^{t} \exp\left\{ \frac{(1-t^2)}{\pi} \int_{-1}^{1} \frac{\beta(\tau) - \beta(t)}{(\tau - t)(\tau t - 1)} d\tau \right\} \frac{df}{dt} \frac{dt}{t}. \tag{27}$$

The above formal solution contains two arbitrary parameters A and t_o, and an arbitrary real function $\beta(t)$. They are governed by the following conditions. First, application of condition (2) to (23) yields

$$U e^{-i\alpha} = t_o \exp\left\{ -\frac{(1-t_o^2)}{\pi} \int_{-1}^{1} \frac{\beta(\tau)\, d\tau}{(\tau - t_o)(\tau t_o - 1)} \right\}. \tag{28}$$

Next, let us consider the boundary condition on the solid surface. In the case of fixed detachment, the angle β is a given function of s (see (21)). However s(t) and hence $\beta(t) = \beta(s(t))$, which appear in (27) and (28), are

not known á priori. Thus the right-hand side of (27) and (28) may be regarded as two integral operators $\mathcal{I}_1\ [s(t),\ \beta(s);\ t_o\ ]$ and $\mathcal{I}_2\ [\,s(t), \beta(s);\ t_o\ ]$ depending on s(t), $\beta(s)$ and parameter t_o, which provide the functional transformations of s(t) into the left-hand side member of (27) and (28), or symbolically,

$$s(t)/A = \mathcal{I}_1\ [s(t),\ \beta(s(t));\ t_o\ ], \tag{29}$$

$$U e^{-i\alpha} = \mathcal{I}_2\ [s(t),\ \beta(s(t));\ t_o\ ], \tag{30}$$

the right-hand sides of these equations being independent of the parameter A. Equations (29) and (30) are a set of functional equations for the unknowns $s(t;\ t_o)$, $\beta(t)$ and t_o. Finally the parameter A is fixed by the physical scale of the total arc length

$$s(1) = S. \tag{31}$$

For the problem of smooth detachment, each smooth-separation point becomes an additional unknown for which another condition must be imposed for its determination. We may adopt the finite curvature condition that

$$\frac{d\omega}{dt} = 0 \qquad at \qquad t = \mp 1, \tag{32}$$

where $\omega = i \log w$ and where $t = -1$ (or 1) is applicable when the smooth detachment occurs at A (or B). This can be seen as follows. From the local conformal behavior of f(t) at $t = \mp 1$ it is obvious that df/dt vanishes like $(t \pm 1)$ as $|\,t \pm 1\,| \to 0$. Therefore the curvature of the free streamline ($\kappa_c = d\omega/df$, see (25b)) will be infinite at the detachment unless $d\omega/dt$ also vanishes there. In the latter case it follows from Villat's alternative (Villat (1914)) that the curvature of the free streamline at detachment coincides with that of the body. By using (23), condition (32) can further be written

$$\lim_{t \to \pm 1} \left\{ \frac{1}{t} + \frac{1}{\pi} \frac{d}{dt} \int_{-1}^{1} \left(\frac{1}{\tau - t} - \frac{1}{\tau - t^{-1}} \right) \beta(\tau)\, d\tau \right\} = 0, \tag{32a}$$

which must be used together with the previous conditions to determine $\beta(s(t))$, t_o, and A.

The above considerations provide a means of constructing inverse and approximate solutions of the cavity problem. For the inverse problem we begin with an adequate choice of t_o and the function $\beta(t)$, then α and U (or σ) can be calculated directly from (28), and the geometrical configuration by quadrature from (26). Again, the body profile varies for different α and σ. The exact solution of an appropriate inverse problem can also be used as the reference flow for approximate solutions of the original physical problem.

5. Numerical Iteration and Approximate Methods

The general profile of the curved obstacle may admit (N-1) isolated sharp corners across each of which (say at z_k) the inclination β jumps by $(-\epsilon_k \pi)$ so that we may write

$$\beta(s) = -\sum_{k=1}^{N-1} (\epsilon_k \pi) H(s - s_k) + \gamma(s) \qquad (33)$$

where s_k is the arc length from A to z_k, and H is the Heaviside step function. Clearly $\gamma(s)$ is continuous everywhere on the wetted surface. We present in the following two numerical schemes, the first one being entirely general, whereas the second is characteristic for a particular category of profiles.

(5A) An Integral Iteration Method

The following integral iteration method has been developed for the general purpose and has been found to be relatively simple and straightforward to apply. Suppose there exists a known basic flow referred to which the flow in question may be regarded as a (not necessarily small) perturbation. For convenience the basic flow may be chosen as simple as practical; for example, one may choose an inclined flat plate if $\beta(s)$ is everywhere small, or a two-sided wedge spanning the same end points A and B if $\beta(s)$ is moderate or large. The exact solution of the basic flow will be denoted by

$$\beta = \beta^{(0)}(s), \qquad s = s^{(0)}(t; t^{(0)}), \quad t_o^{(0)}, \quad A^{(0)}. \tag{34}$$

The function $\beta^{(o)}(s)$ is of course different from $\beta(s)$ of (33).

Equations (27) and (28) may be rewritten for the iteration scheme as

$$\frac{1}{A^{(n)}} s^{(n)}(t; t_o^{(n)}) = \int_{-1}^{t} \mathcal{E}\left[\beta(s^{(n-1)}(t; t_o^{(n-1)}))\right] \frac{d}{dt}\left[\frac{f(t; t_o^{(n-1)})}{A^{(n-1)}}\right] \frac{dt}{t}, \tag{35}$$

$$t_o^{(n)} = U e^{-i\alpha}\, \mathcal{F}\left[\beta(s^{(n-1)}(t; t_o^{(n-1)}))\right], \tag{36}$$

for $n = 1, 2, 3, \ldots$, where

$$\mathcal{E}\left[\beta(s(t; t_o))\right] \equiv \exp\left\{\frac{(1-t^2)}{\pi}\int_{-1}^{1} \frac{\beta(\tau)-\beta(t)}{(\tau-t)(\tau t-1)}\, d\tau\right\}, \tag{37}$$

$$\mathcal{F}\left[\beta(s(t; t_o))\right] \equiv \exp\left\{\frac{(1-t_o^2)}{\pi}\int_{-1}^{1} \frac{\beta(\tau)\, d\tau}{(\tau-t_o)(\tau t_o-1)}\right\}. \tag{38}$$

Here $\beta(s^{(n)}(t))$ assumes the corresponding value of the prescribed $\beta(s)$ with $s = s^{(n)}(t)$ for $n = 0, 1, 2, \ldots, s^{(o)}(t)$ being provided by the basic flow. Other than this role, the inclination $\beta^{(o)}(s)$ of the basic flow never explicitly enters the iteration calculation. Finally the physical scale factor $A^{(n)}$ of each n will be so chosen that

$$s^{(n)}(1) = S \qquad \text{for} \quad n = 0, 1, 2, \cdots \tag{39}$$

This condition ensures that the total arc length of the wetted surface in each iteration, including the basic flow, remains fixed (see condition (31))

so that the original boundary condition of the prescribed $\beta(s)$ can be applied in the entire interval $0<s<S$. When the set of values $\{t_o^{(n)}\}$ and functions $\{s^{(n)}(t)\}$ tend to definite limits as $n\to\infty$, then this iteration converges to the required solution. In numerical work, estimates of $|s^{(n+1)}/s^{(n)}-1|$ and $|t_o^{(n+1)}/t_o^{(n)}-1|$ provide good indication of the rate of convergence.

In the problem of smooth detachment one also has to apply the same iteration procedure to the additional condition (32a), use of which must yield convergent values of the detachment points if the solution is to be meaningful.

It should be pointed out here that this iteration method is universal so long as the integral operations involved can be carried out and the process is convergent. It therefore includes the special case of step-jump β for polygonal obstacles.

(5B) Polynomial Representation of $\beta(t)$

Let us consider again the general case (33). While the determination of $\beta(t)$ is generally complicated, the values of β are nevertheless prescribed for the fixed detachment points A and B, $\beta(-1)=\beta_A$, $\beta(1)=\beta_B$, say. Hence from (33) γ is also known at $t=\pm 1$, namely

$$\gamma_A=\gamma(-1)=\beta_A, \qquad \gamma_B=\gamma(1)=\beta_B+\pi\sum_{k=1}^{N-1}\epsilon_k. \tag{40}$$

We may next expand the continuous function $\gamma(t)$ into a power series

$$\gamma(t)=\gamma_A\frac{1-t}{2}+\gamma_B\frac{1+t}{2}+\sum_{m=1}^{\infty}\sum_{n=1}^{\infty}\gamma_{mn}\left(\frac{1-t}{2}\right)^m\left(\frac{1+t}{2}\right)^n \tag{41}$$

which satisfies condition (40) and converges uniformly and absolutely for $-1<t<1$. Furthermore, it is noted from (25) that the curvature of the solid surface near the detachment points is

$$\lim_{t\to\pm|1-0|}\kappa_s(t)=\lim_{t\to\pm 1}e^{\lambda(t)}\frac{d\beta/dt}{df/dt}=\lim_{t\to\pm 1}\frac{d\beta/dt}{df/dt}. \tag{42}$$

But it has already been noted that (df/dt) vanishes like $(1 \pm t)$ as $|1 \pm t| \to 0$. Therefore, as long as the curvature of the wetted surface is finite at the detachment, regardless whether the detachment is fixed or smooth, the following two conditions

$$\frac{d\beta}{dt} = \frac{d\gamma}{dt} = O(1 \pm t) \qquad as \quad |1 \pm t| \to 0, \tag{43a}$$

must be satisfied, which, when applied to (41), yield

$$\gamma_B - \gamma_A = \sum_{n=1}^{\infty} \gamma_{1n} = -\sum_{m=1}^{\infty} \gamma_{m1} . \tag{43b}$$

Actually we can carry out the limit in (42) and apply the known curvature conditions at the detachment points; the result will however be omitted here.

An approximate method is obtained by taking a truncated series in (41) with M terms in m and N terms in n. For simplicity we shall describe this method for the special case of no sharp corners, and hence $\beta(s) = \gamma(s)$. Substituting this polynomial in (27) and (28), we obtain

$$\delta(t) = \int_{-1}^{t} \left(\frac{1+t}{1-t}\right)^{\frac{\gamma_A - \gamma_B}{2\pi t}(1-t^2)} exp\left\{ \frac{(1-t^2)}{\pi} \int_{-1}^{1} \frac{\gamma_{MN}(\tau) - \gamma_{MN}(t)}{(\tau - t)(\tau t - 1)} d\tau \right\} \frac{df}{dt} \frac{dt}{t} , \tag{44}$$

$$U e^{-i\alpha} = t_o \left(\frac{t_o - 1}{t_o + 1}\right)^{\frac{\gamma_A - \gamma_B}{2\pi t_o}(1-t_o^2)} exp\left\{ -i\left(\frac{\gamma_A + \gamma_B}{2} + \frac{\gamma_B - \gamma_A}{2t_o}\right) - \frac{(1-t_o^2)}{\pi} \int_{-1}^{1} \frac{\gamma_{MN}(\tau) d\tau}{(\tau - t_o)(\tau t_o - 1)} \right\} \tag{45}$$

where

$$\gamma_{MN}(t) = \sum_{m=1}^{M} \sum_{n=1}^{N} \gamma_{mn} \left(\frac{1-t}{2}\right)^m \left(\frac{1+t}{2}\right)^n . \tag{46}$$

In addition to conditions (44), (45), we have of course conditions (43b) (31) and (32) (the last one being for the smooth detachment case).

In case the change of the surface inclination is sufficiently smooth over the entire surface, especially near the points A and B, one may regard $\gamma^{(o)}(t) = (\gamma - \gamma_{MN})$ as the reference flow and derive a linear problem for the coefficients γ_{mn}. An appropriate number of points on the real t-axis may be chosen for application of condition (44).

6. Lift and Drag

The complex force $F = X + iY$ is seen to be

$$F = i\int_A^B (p - p_c)\,dz = \frac{1}{2} i\rho \int_{CABC'} (1 - w\bar{w})\,dz = -\frac{1}{2} i\rho \oint_\Gamma (1 - w\bar{w}) \frac{dz}{dt}\,dt \tag{47}$$

where the contour Γ is C'BAC. The first term of the last integral becomes

$$F_1 = -\frac{1}{2} i\rho \oint_\Gamma \frac{1}{w} \frac{df}{dt}\,dt = \frac{1}{2} i\rho \oint_\Gamma f \frac{d}{dt}\left(\frac{1}{w}\right) dt$$

by integration by parts; and the complex conjugate of the second integral is

$$\overline{F_2} = \frac{1}{2} i\rho \int_{CABC'} w\bar{w}\,d\bar{z} = \frac{1}{2} i\rho \int_{CABC'} w\,df = \frac{1}{2} i\rho \oint_\Gamma f \frac{dw}{dt}\,dt,$$

Now the integrand of the last two integrals are analytic and regular everywhere inside the contour Γ except at the simple pole $t = t_o$. Since as $t \to t_o$,

$$f(t) = \frac{B}{t - t_o} + O(1), \qquad B = \frac{A t_o^3 \bar{t}_o}{(t_o - \bar{t}_o)(t_o^2 - 1)(t_o \bar{t}_o - 1)}, \tag{48}$$

we obtain by the theorem of residues

$$F = F_1 + F_2 = -\pi\rho \left\{ B \left[\frac{d}{dt}\left(\frac{1}{w}\right) \right]_{t=t_0} + \bar{B} \overline{\left[\left(\frac{dw}{dt}\right)_{t=t_0} \right]} \right\}$$

$$= \pi\rho\, e^{i\alpha} \left\{ \frac{B}{U} \left(\frac{d \log w}{dt} \right)_{t=t_0} - \bar{B} U \overline{\left(\frac{d \log w}{dt} \right)_{t=t_0}} \right\} \tag{49}$$

by using (2). Finally the lift L and drag D are given by

$$D + iL = F e^{-i\alpha} = \pi\rho \left\{ \frac{B}{U} G(t_0) - U \bar{B}\, \overline{G(t_0)} \right\} \tag{50}$$

where G(t) = d log w/dt, and hence for the polygonal obstacles

$$G(t) = \frac{1}{t} + \sum_{k=1}^{N-1} \epsilon_k \frac{1-\tau_k^2}{(t-\tau_k)(1-\tau_k t)}\,; \tag{50a}$$

and in general

$$G(t) = \frac{1}{t} + \frac{1}{\pi} \int_{-1}^{1} \left[\frac{1}{(\tau - t)^2} + \frac{1}{(\tau t - 1)^2} \right] \beta(\tau)\, d\tau\,. \tag{50b}$$

7. Some Basic Features of the Free Streamlines

The shape of the free streamlines AC and BC' will now be determined. On the boundary AC and BC' of the near-wake,

$$t = e^{-i\chi}, \qquad 0 < \chi < \pi, \tag{51}$$

which corresponds to $\zeta = \xi = \cos\chi$. Then from (23) and (24b),

$$\omega = i \log w = (\cos^{-1}\xi) + \frac{2}{\pi}(1-\xi^2)^{1/2} \int_{-1}^{1} \frac{\beta(\tau)\, d\tau}{\tau^2 - 2\xi\tau + 1}, \qquad |\xi| < 1. \tag{52}$$

Let the image point of $z = \infty$ be

$$t_0 = V e^{-i\alpha_0}, \qquad \text{with} \quad 0<V<1, \quad 0<\alpha_0<\pi, \tag{53a}$$

or $$\zeta_0 = \xi_0 + i\eta_0, \quad \xi_0 = \tfrac{1}{2}\left(\tfrac{1}{V}+V\right)\cos\alpha_0, \quad \eta_0 = \tfrac{1}{2}\left(\tfrac{1}{V}-V\right)\sin\alpha_0, \tag{53b}$$

with $|\xi_0| < 1$ for the fully developed wake flows. Then on AC and BC',

$$f = \frac{A}{4}\left[(\xi-\xi_0)^2+\eta_0^2\right]^{-1}. \tag{54}$$

The curvature of AC and BC', by (25b), is $\kappa_C = d\omega/df$, or

$$\kappa_C = \frac{2}{A}\,\frac{\left[(\xi-\xi_0)^2+\eta_0^2\right]^2}{(\xi-\xi_0)}\left\{(1-\xi^2)^{-1/2} - \frac{2}{\pi}\frac{d}{d\xi}\int_{-1}^{1}\frac{(1-\xi^2)^{1/2}\beta(\tau)\,d\tau}{\tau^2-2\xi\tau+1}\right\}. \tag{55}$$

Thus the curvature of AC and BC' is in general singular at A, B, C and C'. The singular behavior of the curvature at C and C', or at $\zeta = \xi_0$, is an intrinsic feature of this wake model.

A parametric representation of the free boundary AC and BC' can be obtained from

$$z(\xi) - z_A = \int_{-1}^{\xi}\frac{1}{w}\frac{df}{d\xi}\,d\xi = \frac{A}{2}\int_{-1}^{\xi} e^{i\omega(\xi)}\,\frac{(\xi_0-\xi)\,d\xi}{\left[(\xi_0-\xi)^2+\eta_0^2\right]^2}, \quad -1<\xi<\xi_0, \tag{56a}$$

$$z(\xi) - z_B = \int_{1}^{\xi}\frac{1}{w}\frac{df}{d\xi}\,d\xi = \frac{A}{2}\int_{\xi}^{1} e^{i\omega(\xi)}\,\frac{(\xi-\xi_0)\,d\xi}{\left[(\xi-\xi_0)^2+\eta_0^2\right]^2}, \quad \xi_0<\xi<1, \tag{56b}$$

where $\omega(\xi)$ is given by (52).

8. Examples

In the preceding sections several numerical methods have been de-

veloped for the general purpose of evaluating the direct problems. In order to exhibit the important physical effects of cavity flows past curved bodies and at the same time to carry out these numerical schemes, we consider in the following a few typical examples: (A) symmetric wedges, (B) two-step wedges, (C) flat plate with a flap, (D) inclined circular arc. Case (A) contains only a simple integration; the complete result is presented here for possible adoptions as a reference flow for more complex problems. The general methods can often be considerably simplified for particular cases, such as shown in (B) and (C) where a combined use of the direct and inverse calculations can be made very effective and powerful. As a comparison, the integral iteration method has also been applied to (C). Finally, the circular arc problem is solved by using the integral iteration method, and the results compared with the available experiments.

All the numerical computations have been programmed and carried out on the IBM7090 computer at California Institute of Technology. The errors involved in the computations, if explicitly verified, will be stated at the relevant place.

(8A) Symmetric Wedge

Consider the cavity flow past a symmetrical wedge of half vertex angle $\beta\pi$ as shown in Figure 3. The limiting case of infinite cavity at $\sigma = 0$ is known as Bobyleff's problem; and the problem with arbitrary σ has been worked out with various cavity models, e.g., with Riabouchinsky's model by Plesset and Shaffer (1948 a, b), and Perry (1952), and with the wake model of Joukowsky and Roshko by Roshko (1954). The method given here is essentially not different from that of Roshko who presented the numerical result for one case $\beta\pi = 45^{\circ}$. We derive here the final result in a closed form and present numerical values in a wider range.

By symmetry it is obvious that

$$w = e^{i\pi\beta} t^{2\beta} \tag{57}$$

At $z = \infty$, $w = U$, hence

$$t_o = -iV, \qquad V = U^{1/2\beta} = (1+\sigma)^{-1/4\beta}. \tag{58}$$

consequently, from (10),

$$f = A t^2 (t^2+V^2)^{-1}(t^2+V^{-2})^{-1}. \tag{59}$$

The physical plane is therefore

$$z = \int_o^t \frac{1}{w}\frac{df}{dt}\,dt = \frac{f(t)}{w(t)} + 2\beta e^{-i\pi\beta}\int_o^t t^{-(2\beta+1)} f(t)\,dt. \tag{60}$$

Let the length of one wedge face be ℓ, then

$$\frac{\ell}{A} = \frac{V^2}{(1+V^2)^2} + 2\beta\int_o^1 \frac{t^{1-2\beta}\,dt}{(t^2+V^2)(t^2+V^{-2})} \equiv \Psi(\sigma;\beta). \tag{61}$$

From (48), (50) we readily deduce that $L = 0$ and

$$D = \pi\rho\,\beta A V^2 (1-V^4)^{-1}(U^{-1}-U). \tag{62}$$

The drag coefficient based on the wedge base $b = 2\ell \sin\beta\pi$ is therefore

$$C_D(\sigma;\beta) = \frac{D}{\frac{1}{2}\rho U^2 b} = \frac{\pi\beta}{\sin\pi\beta}\left(\frac{V^{-2\beta}-V^{2\beta}}{V^{-2}-V^2}\right)\frac{(1+\sigma)}{\Psi(\sigma;\beta)}. \tag{63}$$

As $\sigma \to 0$, both U and V tend to unity, and we find the following asymptotic behavior

$$C_D(\sigma;\beta) \sim \frac{4\pi\beta^2 \csc\beta\pi}{1+\delta\beta\,\Psi_2(-\beta)}\left[1+\sigma+O(\sigma^2)\right] \tag{64a}$$

where

$$\Psi_n(x) = \frac{1}{2}\int_o^1 \frac{t^x}{(1+t)^n}\,dt \tag{64b}$$

which can be expressed in terms of the logarithmic derivative of the Γ-function.

The above result of C_D is computed and shown in Figure 4 versus the cavitation number σ for a number of the vertex angles $\beta\pi$. The present theory is found in good agreement with the experimental results of Waid (1957) and of Cox and Clayden (1958).

(8B) Two-Step Symmetric Wedge

Let us consider the cavity flow past a two-step symmetrical wedge with the inclination equal to $\beta\pi$ and $(\beta+\gamma)\pi$ on the first and second leg respectively $(0<\beta<1,\ 0<(\beta+\gamma)<1$, see Figure 3), the flow being again symmetric about the x-axis and the imaginary t-axis. Let $t = \pm\tau$ correspond to the intermediate vertices, then

$$w = e^{i\pi\beta}\, t^{2\beta}\, (t^2-\tau^2)^{\gamma}\, (\tau^2 t^2-1)^{-\gamma}. \tag{65}$$

At $z=\infty$, $w = U$ and $t_o = -iV$, $0<V<1$, hence

$$\mu = (V^2+\tau^2)/(1+\tau^2V^2), \qquad \mu \equiv (U/V^{2\beta})^{1/\gamma}. \tag{66}$$

This equation may also be written

$$\tau^2 = (\mu-V^2)/(1-\mu V^2), \quad \text{or} \quad V^2 = (\mu-\tau^2)/(1-\mu\tau^2). \tag{66a}$$

Since $0<\tau^2<1$ and $0<V^2<1$, we deduce from (66a) that (i) $V^2<\mu<1$ and (ii) $\tau^2<\mu<1$. From (i) it immediately follows that

$$U^{1/2\beta} \lessgtr V \lessgtr U^{1/[2(\beta+\gamma)]} \qquad \text{for } \gamma \gtrless 0 \tag{67}$$

(When γ is negative, $|\gamma|$ is taken to be small compared with β.) This inequality gives the range of V for prescribed $U = (1+\sigma)^{-1/2}$, and β, γ. The inequality (ii) then provides an upper bound for τ^2.

The physical plane is given by

$$z = \int_0^t \frac{1}{w}\frac{df}{dt}\,dt = 2A\,e^{-i\pi\beta}\int_0^t \left(\frac{\tau^2 t^2 - 1}{t^2 - \tau^2}\right)^{\gamma} t^{1-2\beta}\, g(t)\,dt \tag{68a}$$

where
$$g(t) = \frac{1}{2At}\frac{df}{dt} = \frac{(1-t^4)}{(t^2+V^2)^2(t^2+V^{-2})^2} \tag{68b}$$

Let ℓ_1 and ℓ_2 be the length of the segment DP_1 and P_1A, then

$$\int_\tau^1 \left(\frac{1-\tau^2 t^2}{t^2-\tau^2}\right)^{\gamma} t^{1-2\beta} g(t)\,dt = \frac{\ell_2}{\ell_1}\int_0^\tau \left(\frac{1-\tau^2 t^2}{\tau^2 - t^2}\right)^{\gamma} t^{1-2\beta} g(t)\,dt. \tag{69}$$

The width of the wedge base is

$$\ell_{AB} = 2\left[\ell_1 \sin\beta\pi + \ell_2 \sin(\beta+\gamma)\pi\right] = 4A\,F(\tau, V), \tag{70a}$$

$$F(\tau, V) = \left[\sin\beta\pi + \frac{\ell_2}{\ell_1}\sin(\beta+\gamma)\pi\right]\int_0^\tau \left(\frac{1-\tau^2 t^2}{\tau^2 - t^2}\right)^{\gamma} t^{1-2\beta} g(t)\,dt. \tag{70b}$$

For given β, γ, σ, ℓ_2/ℓ_1, the parameters V and τ can be determined from (66) and (69). If use is made of (66a) in expressing $\tau = \tau(V)$, one can compute V directly from (69) as a function of $\beta, \gamma, \sigma, \ell_2/\ell_1$.

Finally, application of (50) to this case gives that L = 0, and

$$D = A\pi\rho\,\frac{U^{-1} - U}{V^{-2} - V^2}\left\{\beta + \gamma\,\frac{(1-\tau^4)V^2}{(\tau^2+V^2)(1+\tau^2 V^2)}\right\}. \tag{71}$$

Therefore the drag coefficient based on the base width is

$$C_D = \frac{D}{\frac{1}{2}\rho U^2 \ell_{AB}} = \frac{\pi}{2U^2}\,\frac{U^{-1} - U}{V^{-2} - V^2}\left\{\beta + \gamma\,\frac{(1-\tau^4)V^2}{(\tau^2+V^2)(1+\tau^2 V^2)}\right\}\frac{1}{F(\tau, V)}. \tag{72}$$

A very straightforward scheme is adopted for the numerical computation in this case. For prescribed cavitation number σ (and hence

U), a set of values of V are chosen within the region of (67), each of which then gives a fixed τ by (66a). The ratio ℓ_2/ℓ_1 can therefore be calculated from (69) as a function of (U, V; β, γ) from which it readily follows the result of C_D by (72). No further elaboration is needed here as the numerical work involved is rather simple. The drag coefficient C_D is shown versus $\ell_2/(\ell_1+\ell_2)$ with fixed values of σ in Figures 5, 6, 7 for three special cases: $\beta\pi = \gamma\pi = 30^\circ$, 45° and 90°. The last case has also been considered by Plesset and Perry (1954). The agreement between the present theory and the experiment of Waid (1957) may be regarded to be good, as shown in an inserted cross plot of Figure 7. The result that Waid's data are all slightly higher than the theory for $b/a = \infty$ (for which case the flow is almost all stagnant inside the cup) may be due to the intrinsic feature of this flow model, or the wall effect which was not accounted for originally.

(8C) Flat Plate with a Flap

As the simplest case of a polygonal obstacle in an asymmetrical flow we consider a flat plate AP_1 with an extended flap P_1B held at a flap angle $\epsilon\pi$ which will be taken positive here (see Figure 3). With the x-axis taken along AP_1, we have

$$w = t\,(t-\tau)^{\epsilon}(\tau t-1)^{-\epsilon}, \tag{73}$$

where $t = \tau$ is the image of the point P_1. At $z = \infty$, $w = Ue^{-i\alpha}$, $t = t_o$, hence

$$t_o = Ue^{-i\alpha}(1-\tau t_o)^{\epsilon}(\tau - t_o)^{-\epsilon}. \tag{74}$$

From this equation it is readily seen that $U < |t_o| < 1$ (or see (13a)).

The physical plane is given by

$$z(t) = 2A\int_{-1}^{t}\left(\frac{\tau t-1}{t-\tau}\right)^{\epsilon} g(t;t_o)\,dt \tag{75a}$$

where

$$q(t;t_o)=\frac{1}{2At}\frac{df}{dt}=\frac{(1-t^2)\left[1+t^2-\frac{1}{2}t\,(t_o+\bar{t}_o)(1+t_o^{-1}\bar{t}_o^{-1})\right]}{(t-t_o)^2(t-\bar{t}_o)^2(t-t_o^{-1})^2(t-\bar{t}_o^{-1})^2}. \tag{75b}$$

Let C and f_* be respectively the unflapped chord and the flap length. Then

$$\int_{-1}^{\tau}\left(\frac{1-\tau t}{\tau-t}\right)^{\epsilon}q(t;t_o)\,dt=\left(\frac{c}{f_*}-1\right)\int_{\tau}^{1}\left(\frac{1-\tau t}{t-\tau}\right)^{\epsilon}q(t;t_o)\,dt. \tag{76}$$

For the convenience of computation, (76) can be written by change of variables,

$$\int_0^1\frac{q(t_1(u);t_o)}{u^{\epsilon}(1-\tau u)^2}\,du=\left(\frac{c}{f_*}-1\right)\int_0^1\frac{q(t_2(u);t_o)}{u^{\epsilon}(1+\tau u)^2}\,du \tag{77a}$$

where

$$t_1(u;\tau)=\frac{\tau-u}{1-\tau u},\qquad t_2(u;\tau)=\frac{\tau+u}{1+\tau u}. \tag{77b}$$

Finally, we derive from (50) for this case the lift and drag as

$$L=\frac{\pi\rho A(U^{-1}+U)\csc\alpha_o}{2(V^{-2}+V^2-2\cos 2\alpha_o)}\left\{\cos\alpha_o+\epsilon\frac{(1-\tau^2)\left[(1+\tau^2)V^2\cos\alpha_o-\tau V(1+V^2)\cos 2\alpha_o\right]}{(V^2+\tau^2-2V\tau\cos\alpha_o)(1+V^2\tau^2-2V\tau\cos\alpha_o)}\right\}, \tag{78a}$$

$$D=\frac{\pi\rho A(U^{-1}-U)/(1-V^2)}{2(V^{-2}+V^2-2\cos 2\alpha_o)}\left\{1+V^2+\epsilon\frac{(1-\tau^2)\left[(1+\tau^2)V^2(1+V^2)-2\tau V(1+V^4)\cos\alpha_o\right]}{(V^2+\tau^2-2V\tau\cos\alpha_o)(1+V^2\tau^2-2V\tau\cos\alpha_o)}\right\} \tag{78b}$$

where $t_o = Ve^{-i\alpha_o}$.

Equations (74) and (76) are two equations for t_o and τ which can be solved numerically for prescribed U, α, ϵ and f_*/c. In the numerical computation the following different schemes have been adopted. The very nature of this special problem permits a combined use of iteration and the inverse problem calculation. If we choose U, α, ϵ and τ as the independent parameters (which are a mixture of the physical and inverse parameters), then t_o can be obtained from (74) by iteration*

$$t_o^{(n)} = U e^{-i\alpha} \mathcal{F}(t_o^{(n-1)}; \tau, \epsilon) \qquad \text{for } n=1,2,\cdots, \tag{79a}$$

where

$$\mathcal{F}(t_o; \tau, \epsilon) = (1-\tau t_o)^{\epsilon} (\tau - t_o)^{-\epsilon}, \tag{79b}$$

and $t_o^{(o)}$ may be chosen to be $Ue^{-i\alpha}$. This computation was programmed for an IBM7090 electronic computer, and the iteration executed until the error of $|t_o^{(n)} - t_o^{(n-1)}| < 0.0001$ is obtained. The convergence of this iteration is found to be very fast. With a series of τ chosen in $-1 < \tau < 1$, and with t_o so determined, the remaining parameter f_*/c can then be determined readily from (76) or (77), and the lift and drag from (78). The accuracy of f_*/c and L, D depends on the $t_o^{(n)}$ used in the calculation, but otherwise their errors have not been explicitly determined by using two consecutive values of $t_o^{(n)}$. The numerical results of C_L and C_D (based on the chord c) are first plotted versus f_*/c (with the * deleted) for a set of values of σ and $\epsilon\pi$, as shown in Figures 8 a - g. From these figures the variation of C_L and C_D with σ can be obtained by cross-plotting, a typical case of $f/c = 0.2$ being given in Figure 8. The special case of this problem with $\sigma = 0$ has recently been treated by Lin (1961) using Levi-Civita's method. The corresponding numerical results of these two cases are found in perfect agreement.

It is easy to see that the above method (with τ_k chosen in order to calculate ℓ_k) soon becomes impractically complicated with further increase in the number of polygonal faces. For the purpose of comparison, this problem has also been calculated by applying the general integral

* The iteration method is used here for the purpose of testing the rate of convergence.

iteration method as described in Section (5A) which has been carried out on the IBM7090 computer. It has been found that to obtain the same accuracy, the computer time for the integral iteration method is considerably more than that for the method mentioned above. It is felt, however, that the integral iteration method will be likely more advantageous and time-saving when there are more than two consecutive flaps.

(8D) Circular Arc Hydrofoil

As an example of the general profile with continuously varying inclination, we consider the circular arc hydrofoil with radius R and arc length $2\gamma R$ so that the arc angle is 2γ (see Figure 9). The inclination β is a linear function of s:

$$\beta(s) = \gamma - \frac{s}{R}, \qquad 0 < s < 2\gamma R. \tag{80}$$

The problem has previously been treated by Wu (1956a) adopting the wake model of Joukowsky and Roshko and using Levi-Civita's method in an approximate manner such that the series expansion is truncated and the boundary conditions on the inclination and curvature are satisfied only at the end points. The numerical work was carried out for $\gamma = 8^{\circ}$ and the results compared with the experiments of Parkin (1956). The case of small γ has also been considered by Wu (1956b) as an example of the generalization of Tulin's linearized theory (1955). These two linear and non-linear theories have been compared for the case $\gamma = 8^{\circ}$ (see Wu, 1956b).

In order to compare the present cavity flow theory and the associated computational program with the previous nonlinear theory (Wu, 1956a), the numerical work of this problem has been carried out for $\gamma = 8^{\circ}$, using the integral iteration method of Section (5A) on an IBM7090 computer. In the computer program used in this case the conventional averaged-iteration process is employed. The iteration process is executed until the error of $\left|V^{(n)} - V^{(n-1)}\right|$ and $\left|a_o^{(n)} - a_o^{(n-1)}\right|$ are both less than 0.0001. The convergence of the iteration is considered to be very satisfactory. The resulting C_L and C_D (based on chord length $\ell_{AB} = 2R \sin\gamma$) are shown versus α in Figures 9 and 10, in which Parkin's experimental

data (1956) are included for comparison. The C_D is found to be virtually identical with the previous approximate theory (Wu, 1956a), whereas C_L of the present theory is slightly greater than the previous one for moderate values of σ.

This work was supported by the U. S. Office of Naval Research under Contract Nonr 220 (35). The assistance rendered by Mrs. Z. Harrison, Miss C. Lin and Mrs. M. Goodwin in preparing the manuscript is greatly appreciated.

REFERENCES

Birkhoff, G., Goldstine, H. H. and Zarantonello, E. H., 1954 Rend. Sem. Mat. Torino 13, 205-23.

Birkhoff, G. and Zarantonello, E. H., 1957 Jets, Wakes and Cavities, Academic Press Inc., New York.

Cox, A. and Clayden, W. 1958 Cavitating flow about a wedge at incidence. J. Fluid Mech. 3, 615-37.

Gilbarg, D. 1960 Jets and Cavities. Handbuch der Physik, Vol. IX, 311-445. Springer-Verlag. Berlin.

Leray, J. 1934 C. R. Acad. Sci. Paris 199, p. 1282.

Leray, J. 1935 Les problèmes de représentation conforme de Helmholtz. Comment. Math. Helv. 8, 149-80, 250-63.

Levi-Civita, T. 1907 Scie e leggi di resistenzia. Rend. cir mat. Palermo, 1-37.

Lin, J. D. 1961 A free streamline theory of flows about a flat plate with a flap at zero cavitation number, Tech. Rept. 119-3, Hydronautics, Inc., Rockville, Md.

Parkin, B. R. 1956 Experiments on circular-arc and flat-plate hydrofoils in non-cavitating and full cavity flows. Hydro. Lab. Rept. 47-7, Calif. Inst. Tech. (see also 1958, J. Ship Res. 1, 34-56).

Perry, B. 1952 The evaluation of integrals occurring in the cavity theory of Plesset and Shaffer, Hydro. Lab. Rept. No. 21-11, Calif. Inst. Tech.

Plesset, M. S. and Shaffer, P. A., Jr. 1948a Drag in cavity flow, Rev. Mod. Phys. 20, 228-31.

Plesset, M. S. and Shaffer, P. A., Jr. 1948b Cavity drag in two and three dimensions. J. App. Phys. 19, 934-39.

Plesset, M. S. and Perry, B. 1954 Mémoire sur la mecanique des fluids offerts á M. Dimitri Riabouchinsky, 251-61, Publ. Sci. Tech. Min. de l'Air, Paris.

Roshko, A. 1954 A new hodograph for free streamline theory NACA TN 3168.

Tulin, M. P. 1955 Supercavitating flow past foils and struts. Proc. Symp. on Cavitation in Hydrodynamics, N. P. L. Teddington, London: Her Majesty's Stationary Office.

Villat, H. 1911 Sur la résistance des fluides, Ann. sci. ec. norm. sup. 28, 203-40.

Villat, H. 1914 Sur la validité des solutions de certains problemes d'hydrodynamique. J. de Math. (6) 10, 231-90.

Waid, R. 1957 Water tunnel investigations of two-dimensional cavities, Hydro. Lab. Rept. E-73.6, Calif. Inst. Tech.

Weinstein, A. 1924 Ein hydrodynamischen Unitätssatz Math. Zeit. 19, 265-74.

Weinstein, A. 1927 Sur le théorème d'existence des jets fluids. Rend. d. R. Accad. dei Lincei, p. 157.

Weinstein, A. 1929 Zur theorie der Flüssigkeitsstrahlen. Math. Zeit. 31, 424-33.

Wu, T. Y. 1956a A free streamline theory for two-dimensional fully cavitated hydrofoils. J. Math. Phys. 35, 236-65.

Wu, T. Y. 1956b A note on the linear and nonlinear theories for fully cavitated hydrofoils. Hydro. Lab. Rept. 21-22, Calif. Inst. Tech.

Wu, T. Y. 1962 A wake model for free streamline flow theory, Part I. fully and partially developed wake flows and cavity flows past an oblique flat plate. J. Fluid Mech. 13, 161-181.

APPENDIX

We present here an alternative derivation of the result $w = w(t)$ given by Equation (23) in the text.

The boundary problem of the analytic function $\omega = i \log w = \theta + i\lambda$, which is defined in the upper half ζ-plane (see (7) and Figure 1), may be expressed in terms of $\zeta = \xi + i\eta$ as

$$Im\,\omega = \lambda = 0 \qquad for \qquad \eta = 0, \quad |\xi| < 1, \tag{A1}$$

$$\begin{aligned} Re\,\omega = \theta &= \beta(s) \qquad for \quad \eta = 0, \quad \xi > 1, \\ &= \pi + \beta(s) \qquad for \quad \eta = 0, \quad \xi < -1. \end{aligned} \tag{A2}$$

Here, the function $\beta(s)$, defined by (21b), is assumed to be a known function of ξ. By virtue of (A1) ω can be continued analytically into the lower half ζ-plane by Schwarz's principle of reflection

$$\omega(\bar{\zeta}) = \overline{\omega(\zeta)} \tag{A3}$$

We shall adopt the notation $\omega^{\pm}(\xi) = \theta^{\pm}(\xi) + i\lambda^{\pm}(\xi)$ to signify the limit of ω as $\eta \to \pm 0$, respectively. Then from (A3) it follows that $\theta^{+} = \theta^{-}$, $\lambda^{+} = -\lambda^{-}$. Thus, the original problem given by (A1) and (A2) may also be posed as the following Hilbert problem:

$$\omega^{+} - \omega^{-} = 2i\lambda^{+} = 0 \qquad for \quad |\xi| < 1; \tag{A4}$$

$$\begin{aligned} \omega^{+} + \omega^{-} = 2\theta^{+} &= 2\beta(s(\xi)) \qquad for \quad \xi > 1, \\ &= 2\left[\pi + \beta(s(\xi))\right] \qquad for \quad \xi < -1. \end{aligned} \tag{A5}$$

The general solution of this Hilbert problem can be written (see, for example, Muskhelishvili: Singular Integral Equations (1953), pp 235-8)

$$\omega(\zeta) = \Omega(\zeta)\left\{\frac{1}{\pi}\int_{-\infty}^{-1} \frac{\pi + \beta(s(\xi))}{\sqrt{\xi^2-1}\,(\xi-\zeta)}\,d\xi - \frac{1}{\pi}\int_{1}^{\infty} \frac{\beta(s(\xi))\,d\xi}{\sqrt{\xi^2-1}\,(\xi-\zeta)} + \sum_{n=-\infty}^{\infty} C_n\,\zeta^n\right\} \tag{A6}$$

where $\Omega(\zeta) = i(\zeta^2-1)^{1/2}$, defined with a branch cut from $-\infty$ to -1 and from 1 to ∞ so that $\Omega \to i\zeta$ as $|\zeta| \to \infty$, $0 < \arg\zeta < \pi$, is a solution of the corresponding homogeneous Hilbert problem, and where c_n are arbitrary real coefficients. The solution can be determined uniquely only when the singular behavior of ω is completely specified. For this problem we note that (i) $|\omega| < \infty$ along the free boundary, $\eta = 0$, $|\xi| < 1$, and (ii) $\omega \sim 0(\log\zeta)$ as $|\zeta| \to \infty$, the stagnation point. From these conditions it follows that $c_n = 0$ for all n. Consequently (A6) reduces to the form (23) upon transformation to the t-plane by using (8).

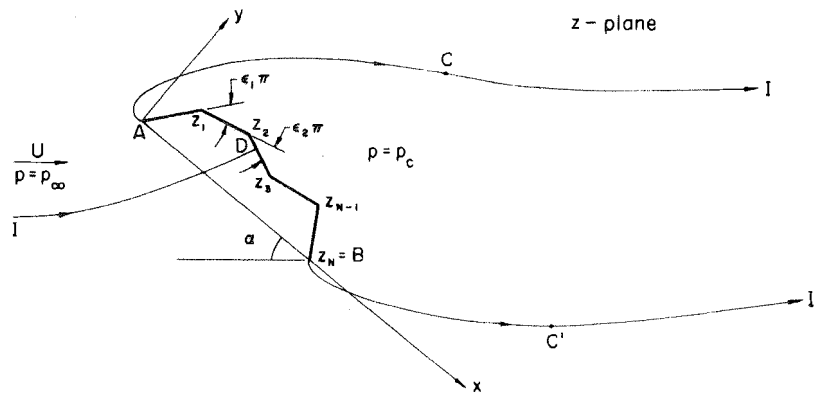

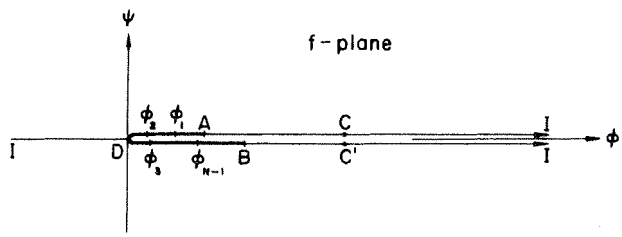

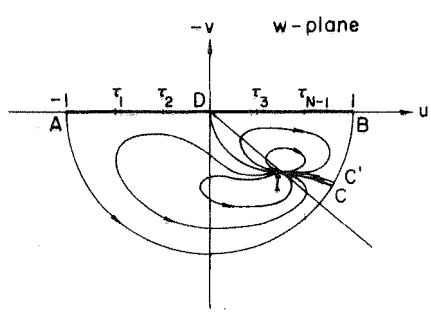

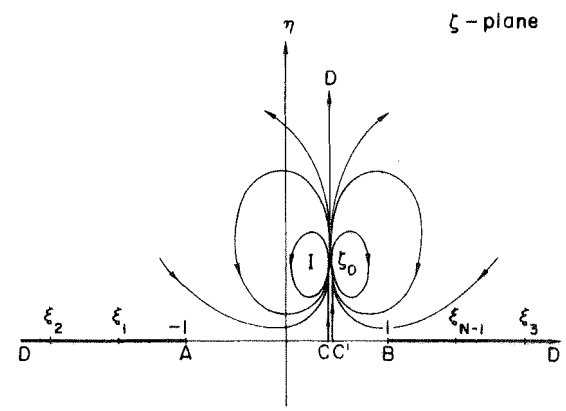

Figure 1. The free-streamline model for the wake flow past a polygonal obstacle and its conformal mapping planes.

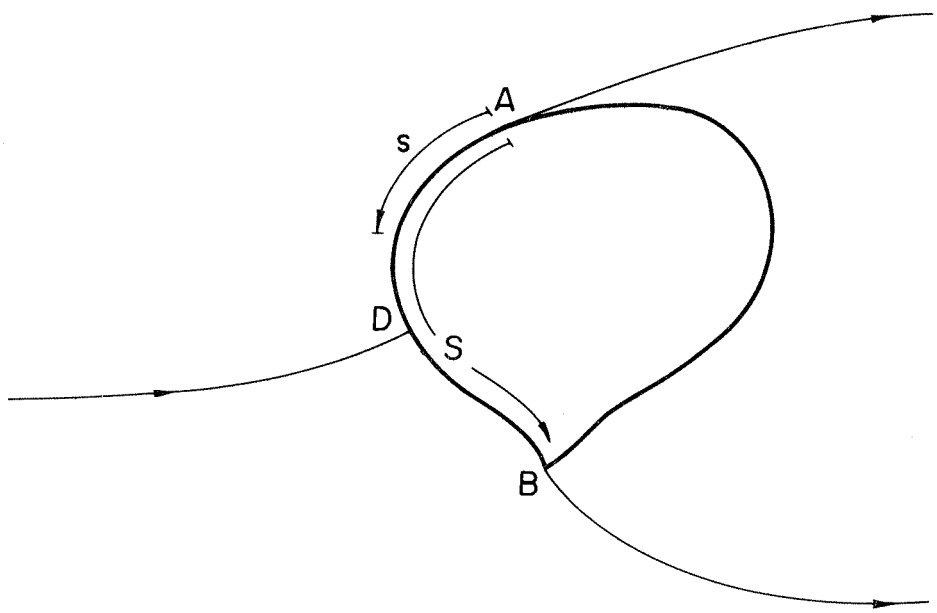

Figure 2. Free-streamlines with fixed and smooth detachment from a solid boundary.

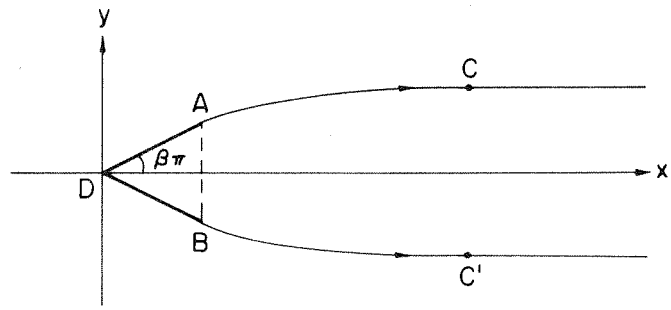

(3a)

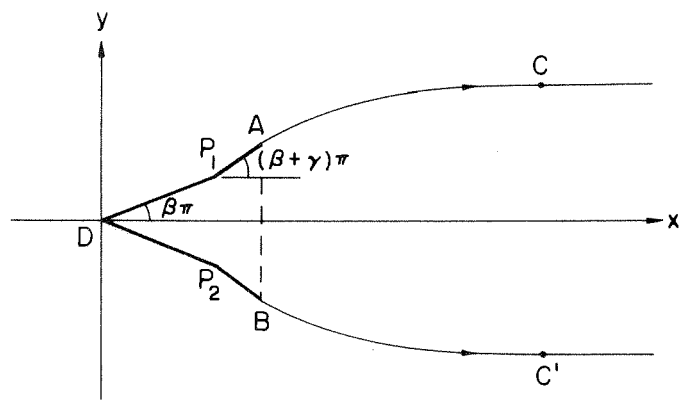

(3b)

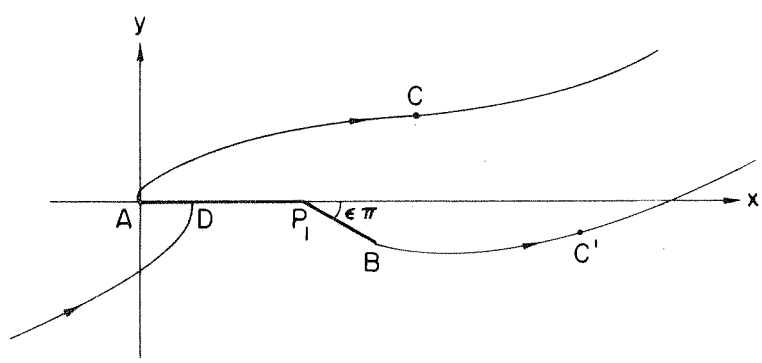

(3c)

Figure 3. The coordinate systems and notations for specific cases.

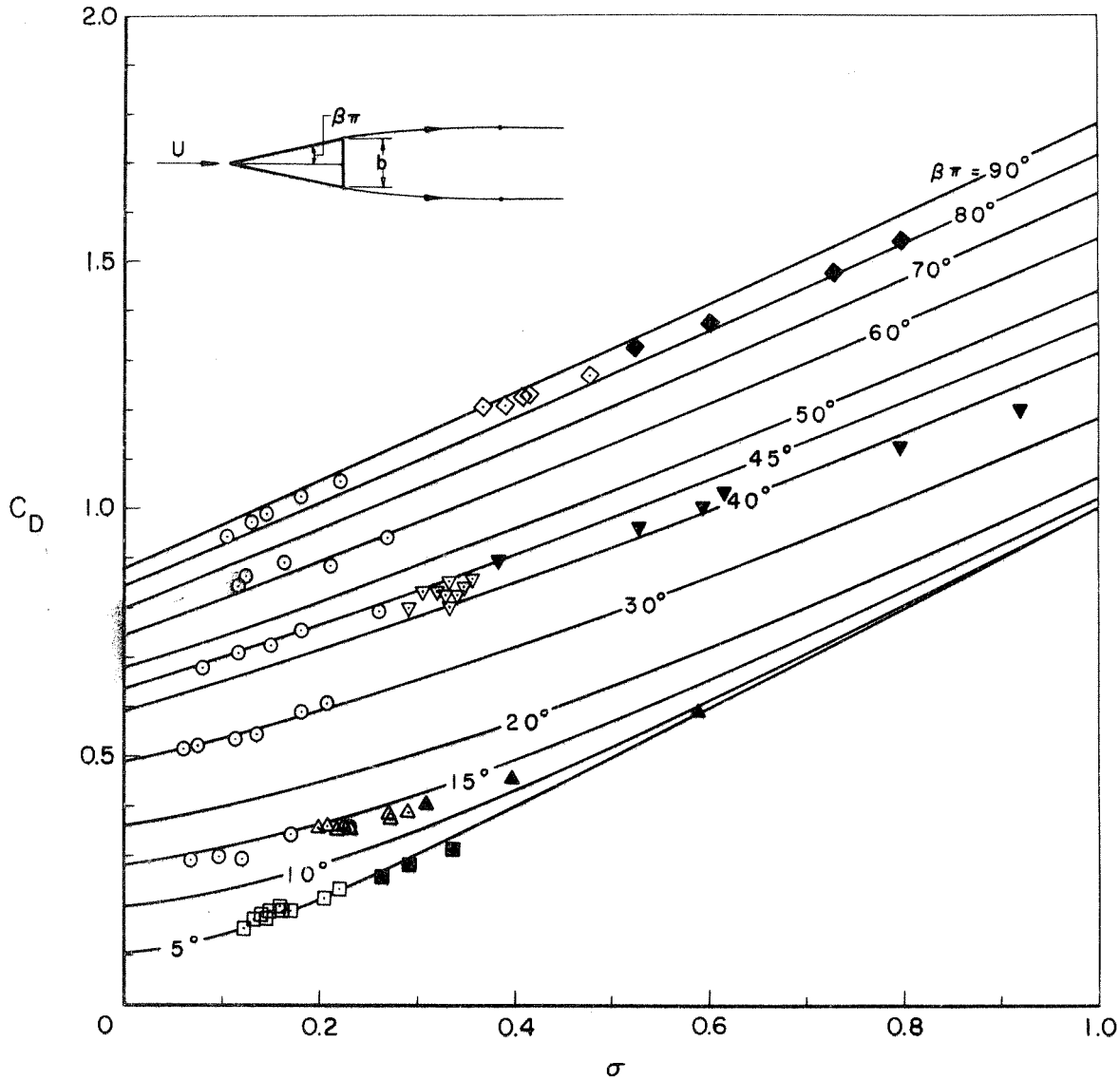

Figure 4. Variation of C_D with the cavitation number σ for symmetric wedges. Waid's data: $\beta\pi = 5^o$, ⊡ ; 15^o, △ ; 45^o, ▽ ; 90^o ◇ ; the solid symbols represent the corresponding data obtained when the cavity was filled with a mixture of water and gas bubbles. Cox and Clayden data: $\beta\pi = 15^o$, 30^o, 45^o, 60^o, 90^o, all represented by ⊙ .

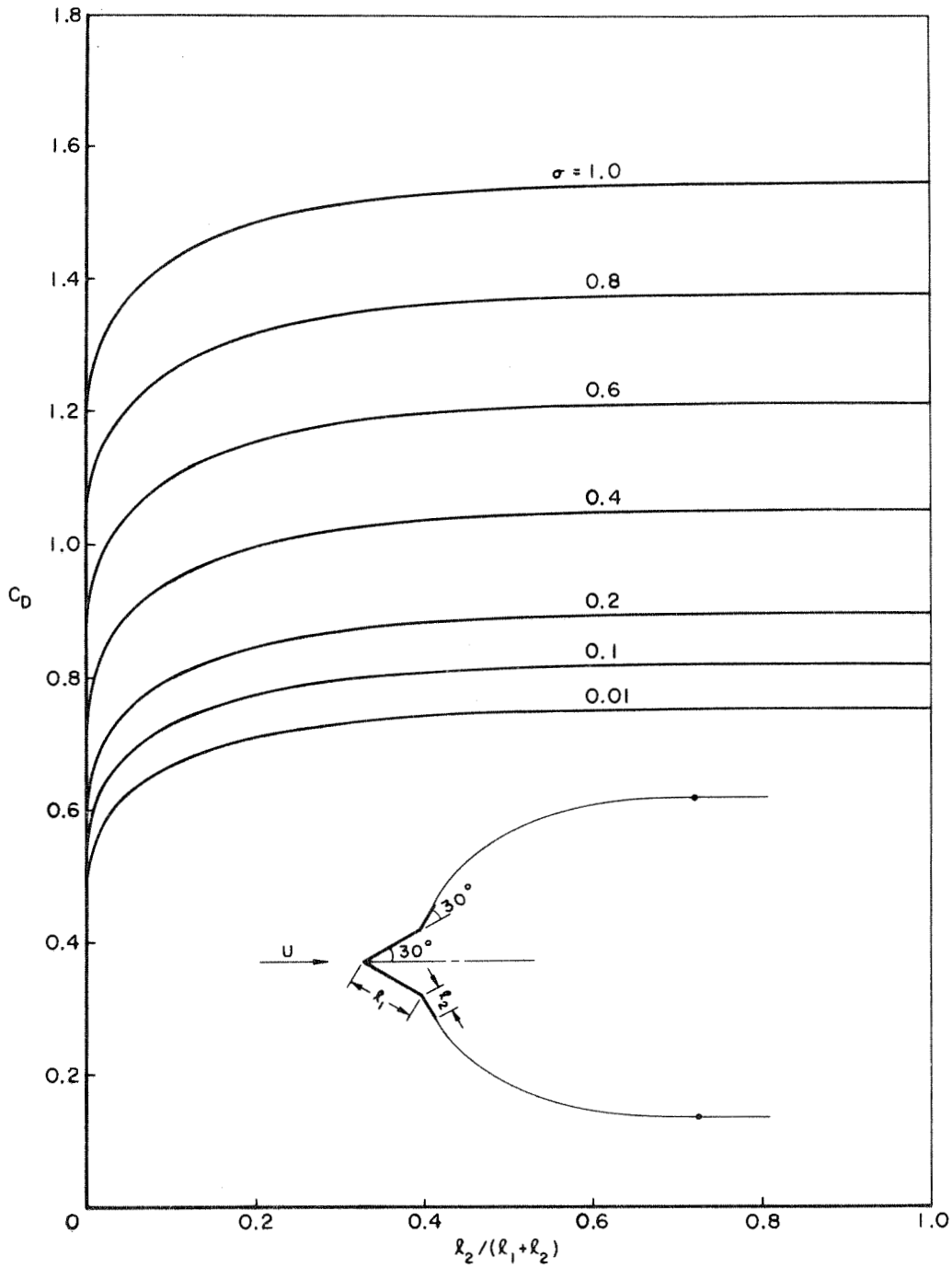

Figure 5. Variation of C_D with $\ell_2/(\ell_1+\ell_2)$ at several values of the cavitation number σ for the two-stepped wedge with $\beta\pi = \gamma\pi = 30^\circ$.

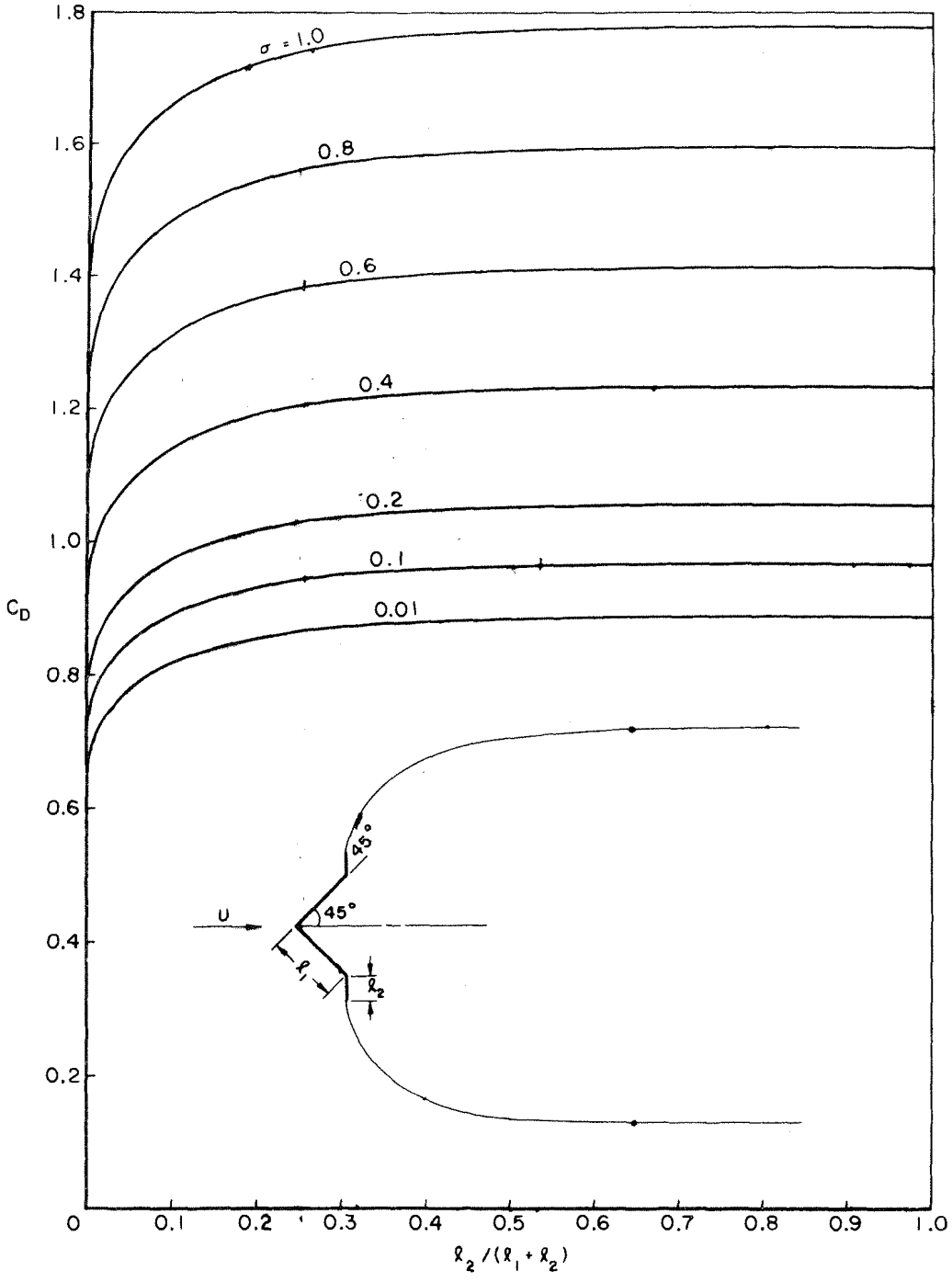

Figure 6. Variation of C_D with $\ell_2/(\ell_1+\ell_2)$ at several values of the cavitation number σ for the two-stepped wedge with $\beta\pi = \gamma\pi = 45^\circ$.

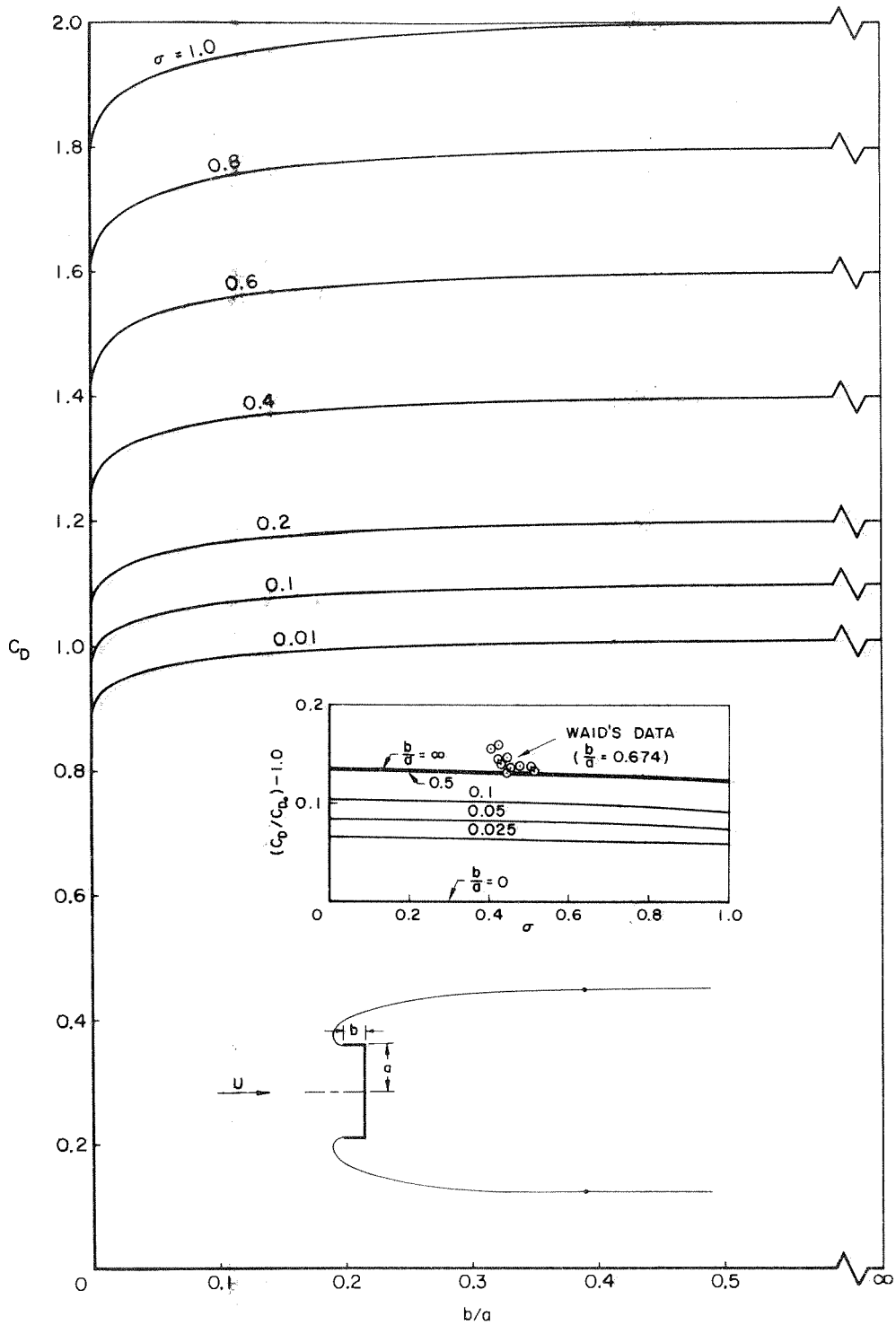

Figure 7. Variation of C_D with b/a at several values of σ for the rectangular cup (or with $\beta\pi = \gamma\pi = 90^\circ$). Waid's data for $b/a = 0.674$ are compared with the theory in the inserted figure.

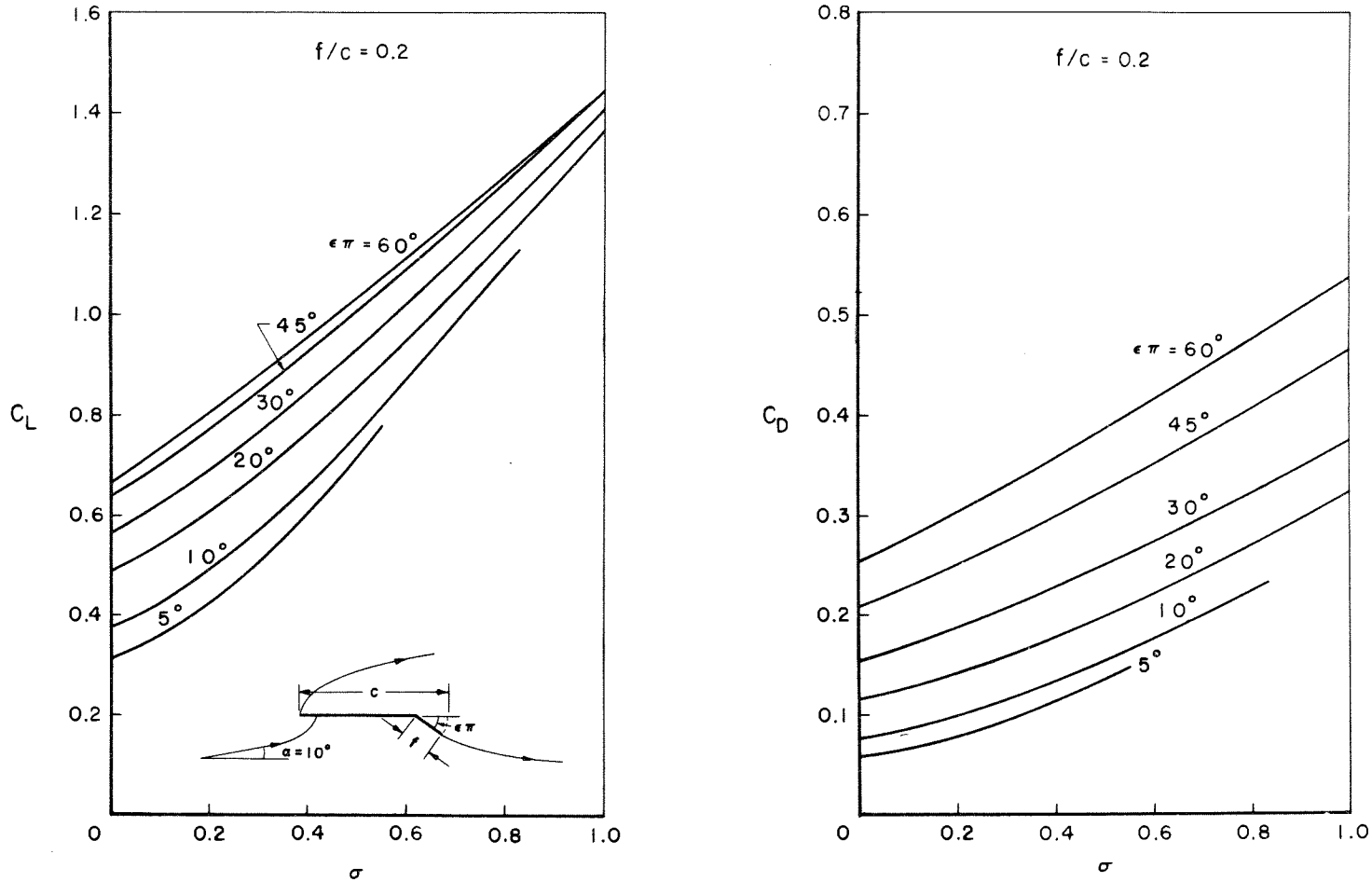

Figure 8. Variation of C_L and C_D with σ for a flap of flap-chord ratio $f/c = 0.2$ incidence $\alpha = 10^o$, with a and held at flap deflection $\epsilon\pi$.

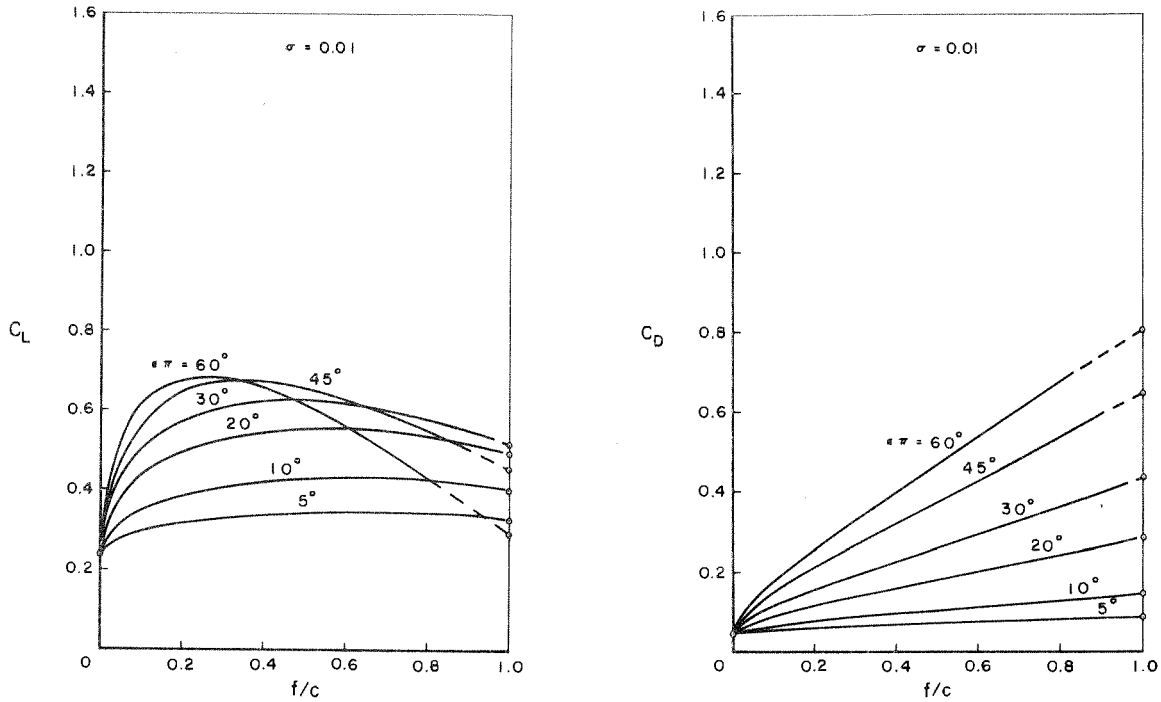

Figure 8(a)

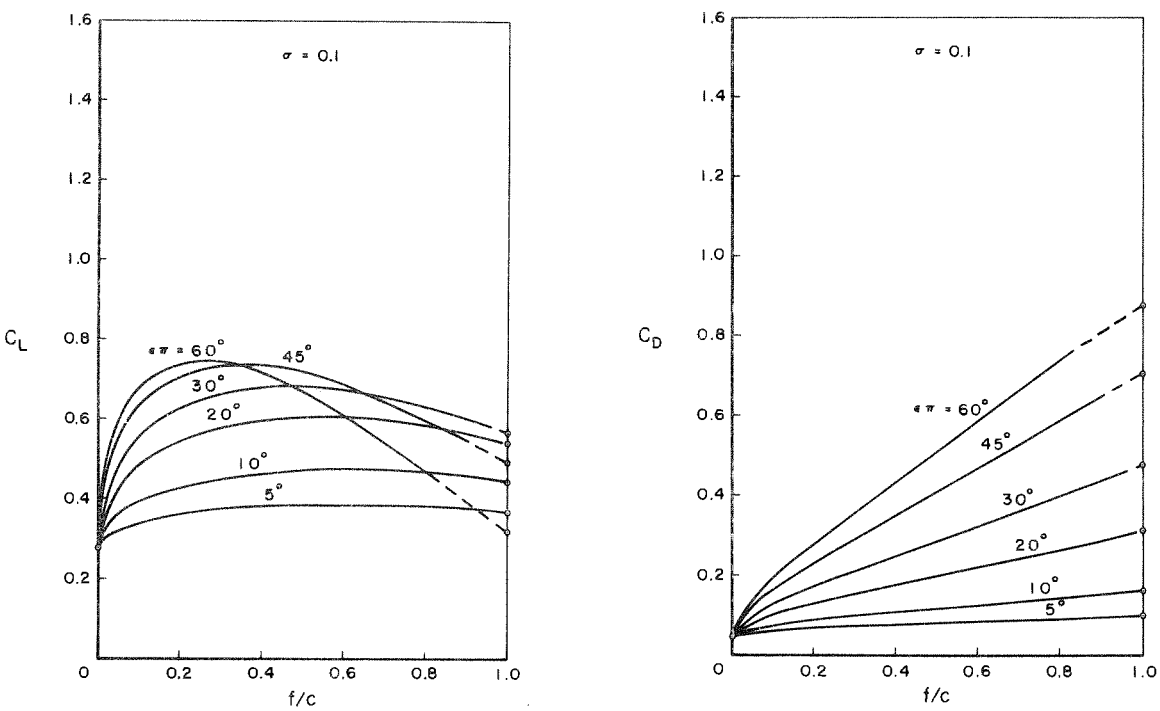

Figure 8(b)

Figure 8(a)-(g) Variation of C_L and C_D with f/c for a flapped plate at $\alpha = 10^o$ shown with several values of σ and $\epsilon\pi$. The symbol ⊙ represents the flat plate solution.

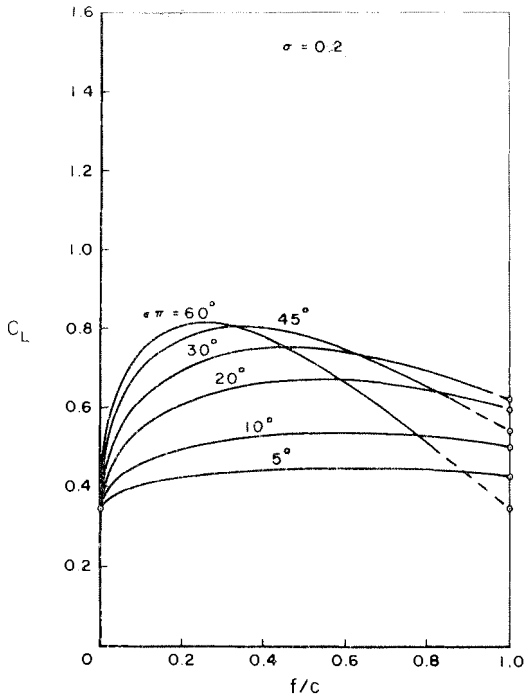

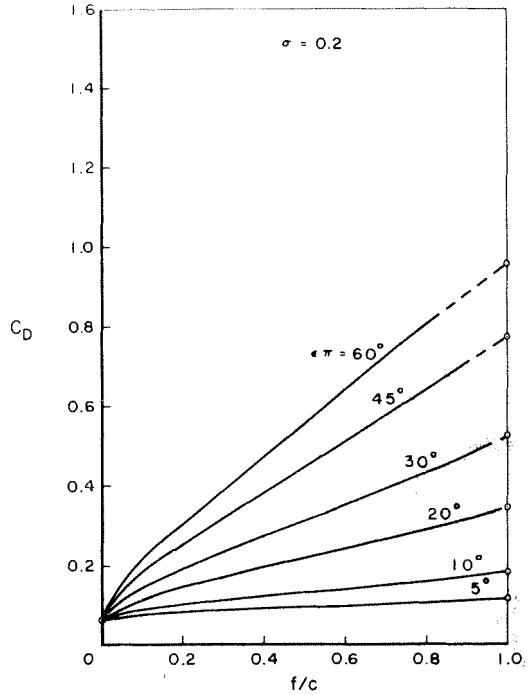

Figure 8(c)

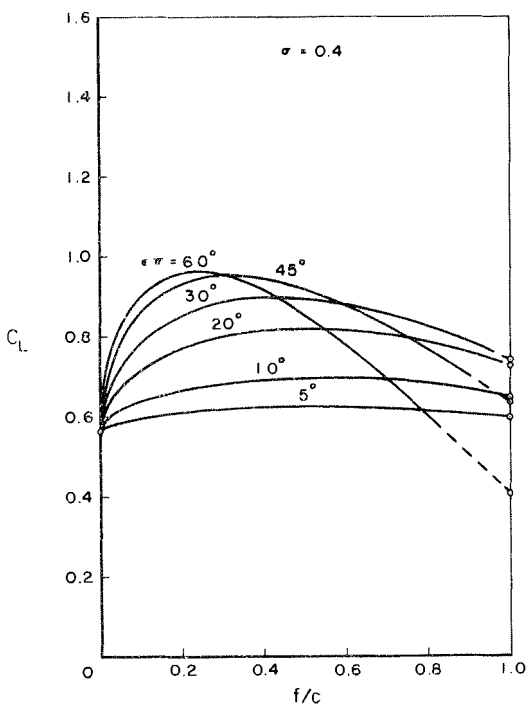

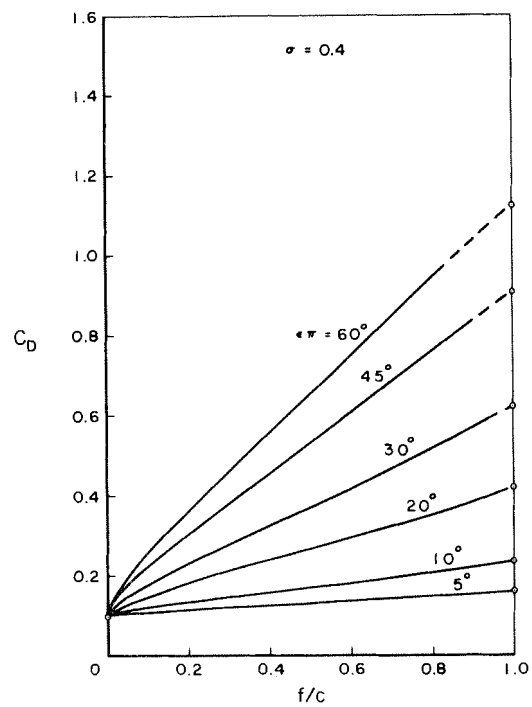

Figure 8(d)

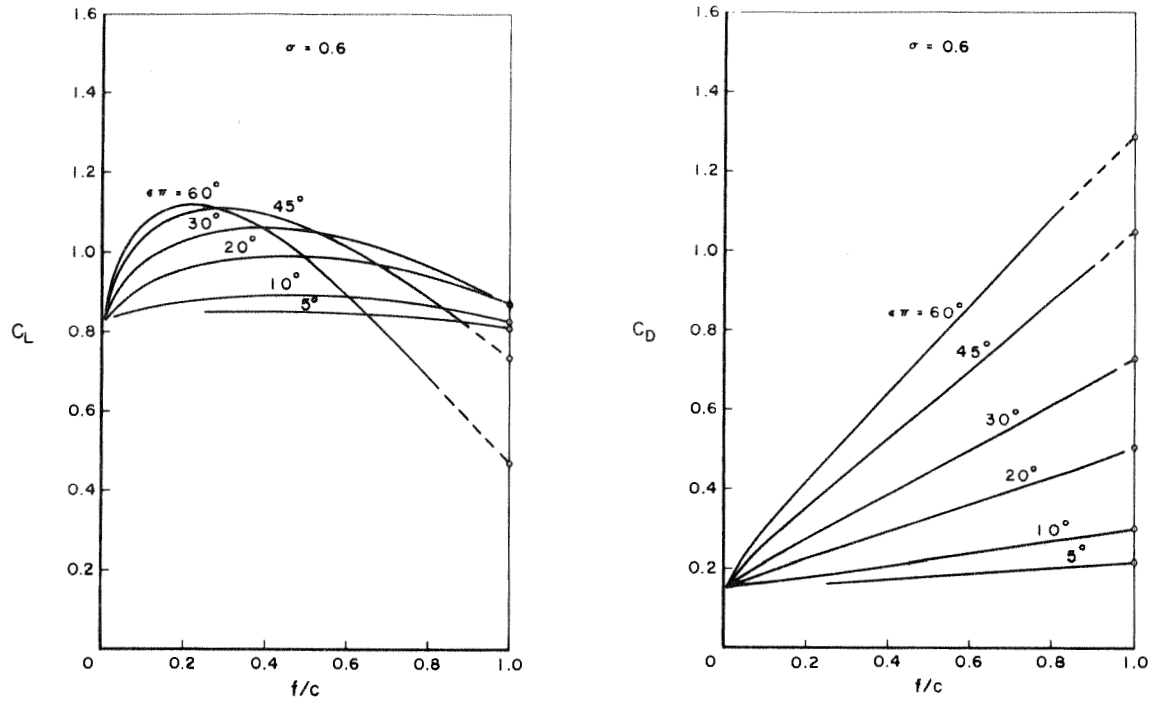

Figure 8(e)

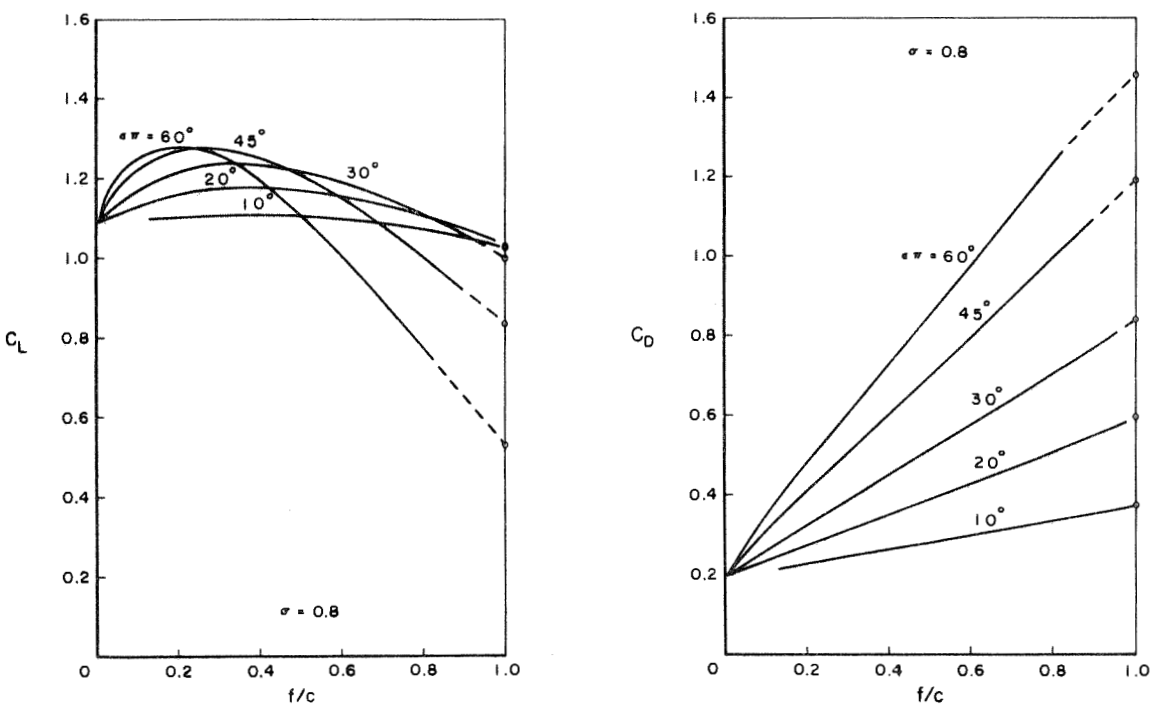

Figure 8(f)

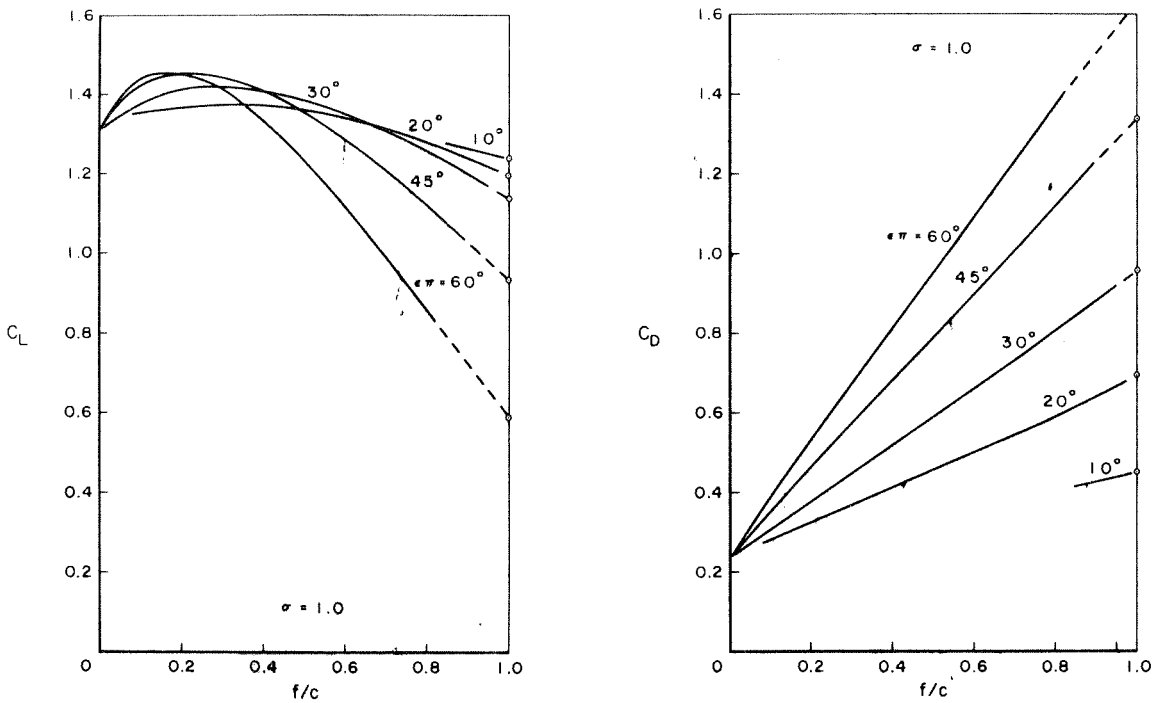

Figure 8(g)

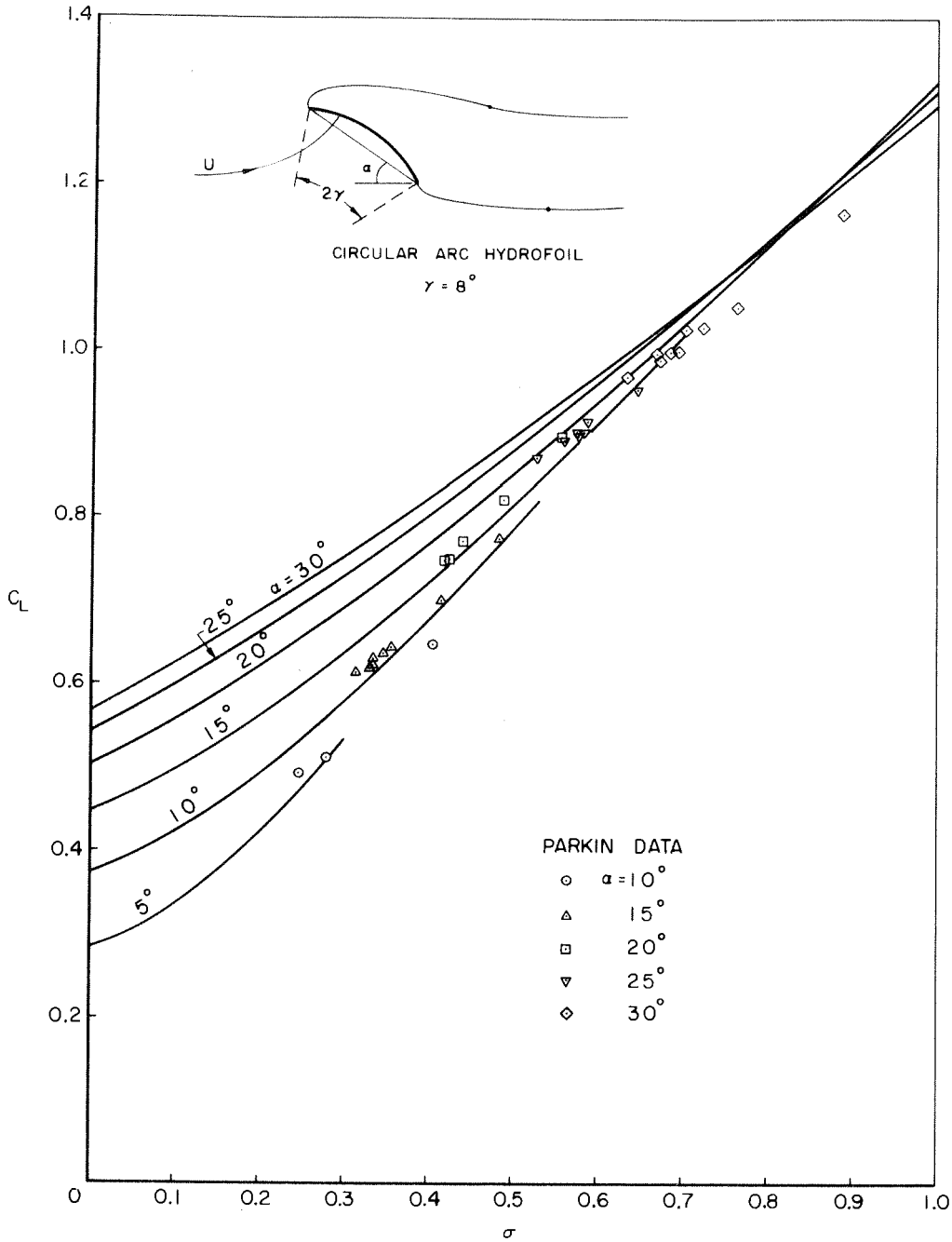

Figure 9. Variation of C_L with σ for a circular arc hydrofoil at incidence α.

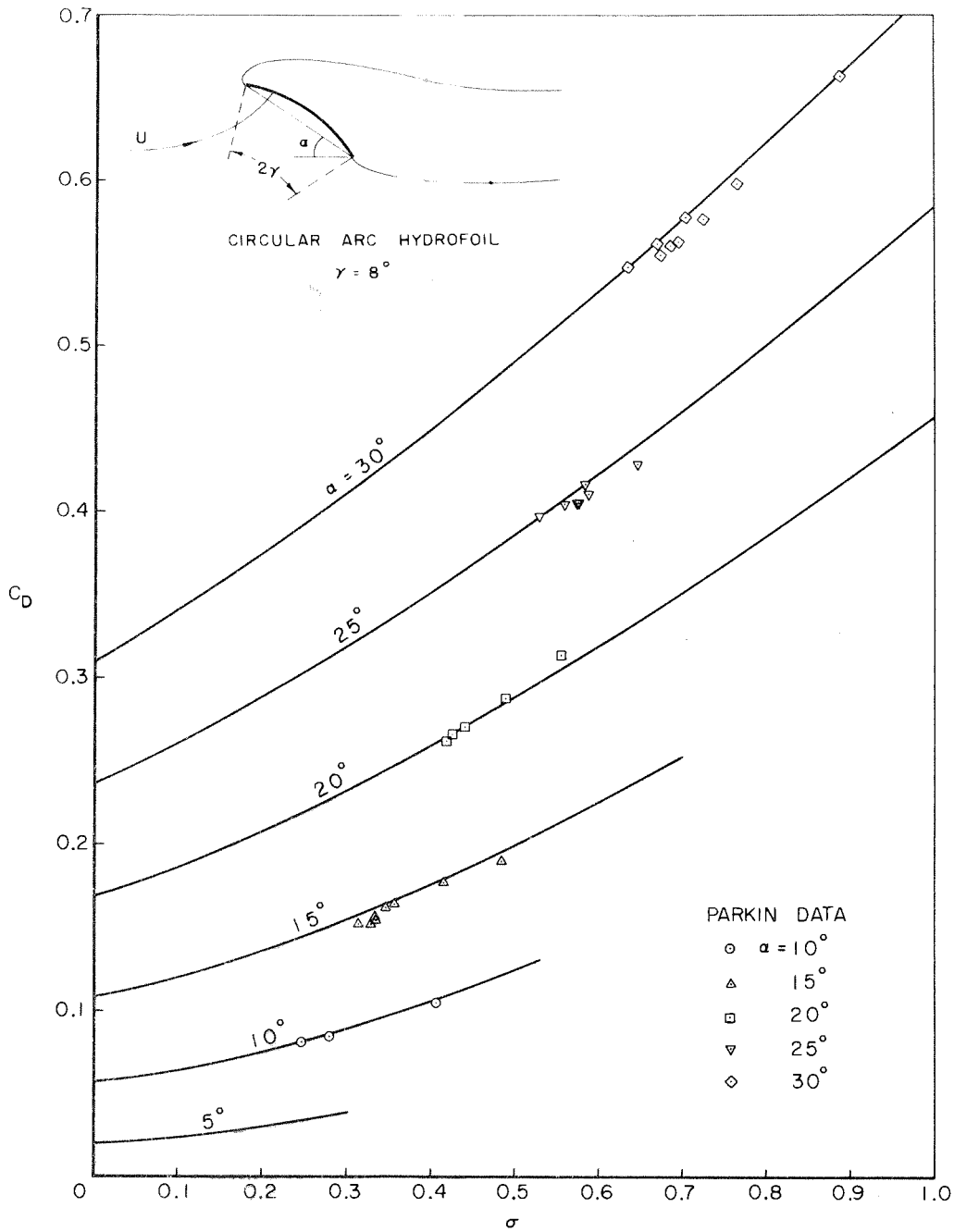

Figure 10. Variation of C_D with σ for a circular arc hydrofoil at incidence α.

DISTRIBUTION LIST FOR UNCLASSIFIED TECHNICAL REPORTS
ISSUED UNDER
CONTRACT Nonr 220(35), TASK NR 062-230
(Single copies unless otherwise specified)

Chief of Naval Research
Department of the Navy
Washington 25, D.C.
Attn: Codes 438 (3)
461
463
466

Commanding Officer
Office of Naval Research
Branch Office
495 Summer Street
Boston 10, Massachusetts

Commanding Officer
Office of Naval Research
Branch Office
207 West 24th Street
New York 11, New York

Commanding Officer
Office of Naval Research
Branch Office
1030 East Green Street
Pasadena, California

Commanding Officer
Office of Naval Research
Branch Office
1000 Geary Street
San Francisco 9, California

Commanding Officer
Office of Naval Research
Branch Office
Box 39, Navy No. 100
Fleet Post Office
New York, New York (25)

Director
Naval Research Laboratory
Washington 25, D. C.
Attn: Code 2027 (6)

Chief, Bureau of Naval Weapons
Department of the Navy
Washington 25, D. C.
Attn: Codes RUAW-r
RRRE
RAAD
RAAD-222
DIS-42

Commander
U. S. Naval Ordnance Test Station
China Lake, California
Attn: Code 753

Chief, Bureau of Ships
Department of the Navy
Washington 25, D. C.
Attn: Codes 310
312
335
420
421
440
442
449

Chief, Bureau of Yards and Docks
Department of the Navy
Washington 25, D. C.
Attn: Code D-400

Commanding Officer and Director
David Taylor Model Basin
Washington 7, D. C.
Attn: Codes 108
142
500
513
520
525
526
526A
530
533
580
585
589
591
591A
700

Commander
U.S. Naval Ordnance Test Station
Pasadena Annex
3202 E. Foothill Blvd.
Pasadena 8, California
Attn: Code P-508

Commander
Planning Department
Portsmouth Naval Shipyard
Portsmouth, New Hampshire

Commander
Planning Department
Boston Naval Shipyard
Boston 29, Massachusetts

Commander
Planning Department
Pearl Harbor Naval Shipyard
Navy No. 128, Fleet Post Office
San Francisco, California

Commander
Planning Department
San Francisco Naval Shipyard
San Francisco 24, California

Commander
Planning Department
Mare Island Naval Shipyard
Vallejo, California

Commander
Planning Department
New York Naval Shipyard
Brooklyn 1, New York

Commander
Planning Department
Puget Sound Naval Shipyard
Bremerton, Washington

Commander
Planning Department
Philadelphia Naval Shipyard
U. S. Naval Base
Philadelphia 12, Pennsylvania

Commander
Planning Department
Norfolk Naval Shipyard
Portsmouth, Virginia

Commander
Planning Department
Charleston Naval Shipyard
U. S. Naval Base
Charleston, South Carolina

Commander
Planning Department
Long Beach Naval Shipyard
Long Beach 2, California

Commander
Planning Department
U. S. Naval Weapons Laboratory
Dahlgren, Virginia

Commander
U. S. Naval Ordnance Laboratory
White Oak, Maryland

Dr. A. V. Hershey
Computation and Exterior
Ballistics Laboratory
U. S. Naval Weapons Laboratory
Dahlgren, Virginia

Superintendent
U. S. Naval Academy
Annapolis, Maryland
Attn: Library

Superintendent
U. S. Naval Postgraduate School
Monterey, California

Commandant
U. S. Coast Guard
1300 E. Street, N. W.
Washington, D. C.

Secretary Ship Structure Committee
U. S. Coast Guard Headquarters
1300 E Street, N. W.
Washington, D. C.

Commander
Military Sea Transportation Service
Department of the Navy
Washington 25, D. C.

U. S. Maritime Administration
GAO Building
441 G Street, N. W.
Washington, D. C.
Attn: Division of Ship Design
Division of Research

Superintendent
U. S. Merchant Marine Academy
Kings Point, Long Island, New York
Attn: Capt. L. S. McCready
(Dept. of Engineering)

Commanding Officer and Director
U. S. Navy Mine Defense Laboratory
Panama City, Florida

Commanding Officer
NROTC and Naval Administrative
Massachusetts Institute of Technology
Cambridge 39, Massachusetts

U. S. Army Transportation Research and
Development Command
Fort Eustis, Virginia
Attn: Marine Transport Division

Mr. J. B. Parkinson
National Aeronautics and Space
Administration
1512 H Street, N. W.
Washington 25, D. C.

Director
Langley Research Center
Langley Station
Hampton, Virginia
Attn: Mr. I. E. Garrick
Mr. D. J. Marten

Director Engineering Sciences Division
National Science Foundation
1951 Constitution Avenue, N. W.
Washington 25, D. C.

Director
National Bureau of Standards
Washington 25, D. C.
Attn: Fluid Mechanics Division
(Dr. G. B. Schubauer)
Dr. G. H. Keulegan
Dr. J. M. Franklin

Defense Documentation Center
Arlington Hall Station
Arlington 12, Virginia (20)

Office of Technical Services
Department of Commerce
Washington 25, D. C.

California Institute of Technology
Pasadena 4, California
Attn: Professor M. S. Plesset
Professor T. Y. Wu
Professor A. J. Acosta

University of California
Department of Engineering
Los Angeles 24, California
Attn: Dr. A. Powell

Director
Scripps Institute of Oceanography
University of California
La Jolla, California

Professor M. L. Albertson
Department of Civil Engineering
Colorado A and M College
Fort Collins, Colorado

Professor J. E. Cermak
Department of Civil Engineering
Colorado State University
Fort Collins, Colorado

Professor W. R. Sears
Graduate School of Aeronautical Engineering
Cornell University
Ithaca, New York

State University of Iowa
Iowa Institute of Hydraulic Research
Iowa City, Iowa
Attn: Dr. H. Rouse
Dr. L. Landweber

Massachusetts Institute of Technology
Cambridge 39, Massachusetts
Attn: Department of Naval Architecture
and Marine Engineering
Professor A. T. Ippen

Harvard University
Cambridge 38, Massachusetts
Attn: Professor G. Birkhoff
(Dept. of Mathematics)
Professor G. F. Carrier
(Dept. of Mathematics)

University of Michigan
Ann Arbor, Michigan
Attn: Professor R. B. Couch
(Dept. of Naval Architecture)
Professor W. W. Willmarth
(Aero. Engineering Department)
Professor M. S. Uberoi
(Aero. Engineering Department)

Dr. L. G. Straub, Director
St. Anthony Falls Hydraulic Laboratory
University of Minnesota
Minneapolis 14, Minnesota
Attn: Mr. J. N. Wetzel
Professor B. Silberman

Professor J. J. Foody
Engineering Department
New York State University Maritime College
Fort Schulyer, New York

New York University
Institute of Mathematical Sciences
25 Waverly Place
New York 3, New York
Attn: Professor J. Keller
Professor J. J. Stoker

The Johns Hopkins University
Department of Mechanical Engineering
Baltimore 18, Maryland
Attn: Professor S. Corrsin
Professor O. M. Phillips (2)

Massachusetts Institute of Technology
Department of Naval Architecture and
Marine Engineering
Cambridge 39, Massachusetts
Attn: Professor M. A. Abkowitz, Head

Dr. G. F. Wislicenus
Ordnance Research Laboratory
Pennsylvania State University
University Park, Pennsylvania
Attn: Dr. M. Sevik

Professor R. C. DiPrima
Department of Mathematics
Rensselaer Polytechnic Institute
Troy, New York

Director
Woods Hole Oceanographic Institute
Woods Hole, Massachusetts

Stevens Institute of Technology
Davidson Laboratory
Castle Point Station
Hoboken, New Jersey
Attn: Mr. D. Savitsky
Mr. J. P. Breslin
Mr. C. J. Henry
Mr. S. Tsakonas

Webb Institute of Naval Architecture
Crescent Beach Road
Glen Cove, New York
Attn: Professor E. V. Lewis
Technical Library

Executive Director
Air Force Office of Scientific Research
Washington 25, D. C.
Attn: Mechanics Branch

Commander
Wright Air Development Division
Aircraft Laboratory
Wright-Pattern Air Force Base, Ohio
Attn: Mr. W. Mykytow, Dynamics Branch

Cornell Aeronautical Laboratory
4455 Genesee Street
Buffalo, New York
Attn: Mr. W. Targoff
Mr. R. White

Massachusetts Institute of Technology
Fluid Dynamics Research Laboratory
Cambridge 39, Massachusetts
Attn: Professor H. Ashley
Professor M. Landahl
Professor J. Dugundji

Hamburgische Schiffbau-Versuchsanstalt
Bramfelder Strasse 164
Hamburg 33, Germany
Attn: Dr. O. Grim
Dr. H. W. Lerbs

Institut fur Schiffbau der
Universitat Hamburg
Berliner Tor 21
Hamburg 1, Germany
Attn: Prof. G. P. Weinblum, Director

Transportation Technical Research Institute
1-1057, Mejiro-Cho, Toshima-Ku
Tokyo, Japan

Max-Planck Institut fur Stromungsforschung
Bottingerstrasse 6/8
Gottingen, Germany
Attn: Dr. H. Reichardt

Hydro-og Aerodynamisk Laboratorium
Lyngby, Denmark
Attn: Professor Carl Prohaska

Shipsmodelltanken
Trondheim, Norway
Attn: Professor J. K. Lunde

Versuchsanstalt fur Wasserbau and
Schiffbau
Schleuseninsel im Tiergarten
Berlin, Germany
Attn: Dr. S. Schuster, Director
Dr. H. Schwanecke
Dr. Grosse

Technische Hogeschool
Institut voor Toegepaste Wiskunde
Julianalaan 132
Delft, Netherlands
Attn: Professor R. Timman

Bureau D'Analyse et de Recherche
Appliquees
47 Avenue Victor Bresson
Issy-Les-Moulineaux
Seine, France
Attn: Professor Siestrunck

Netherlands Ship Model Basin
Wageningen, The Netherlands
Attn: Dr. Ir. J. D. vanManen

National Physical Laboratory
Teddington, Middlesex, England
Attn: Mr. A. Silverleaf, Superintendent
Ship Division
Head, Aerodynamics Division

Head, Aerodynamics Department
Royal Aircraft Establishment
Farnborough, Hants, England
Attn: Mr. M. O. W. Wolfe

Dr. S. F. Hoerner
148 Busteed Drive
Midland Park, New Jersey

Boeing Airplane Company
Seattle Division
Seattle, Washington
Attn: Mr. M. J. Turner

Electric Boat Division
General Dynamics Corporation
Groton, Connecticut
Attn: Mr. Robert McCandliss

General Applied Sciences Labs., Inc.
Merrick and Stewart Avenues
Westbury, Long Island, New York

Gibbs and Cox, Inc.
21 West Street
New York, New York

Lockheed Aircraft Corporation
Missiles and Space Division
Palo Alto, California
Attn: R. W. Kermeen

Grumman Aircraft Engineering Corp.
Bethpage, Long Island, New York
Attn: Mr. E. Baird
Mr. E. Bower
Mr. W. P. Carl

Midwest Research Institute
425 Volker Blvd.
Kansas City 10, Missouri
Attn: Mr. Zeydel

Director, Department of Mechanical Sciences
Southwest Research Institute
8500 Culebra Road
San Antonio 6, Texas
Attn: Dr. H. N. Abramson
Mr. G. Ransleben
Editor, Applied Mechanics Review

Convair
A Division of General Dynamics
San Diego, California
Attn: Mr. R. H. Oversmith
Mr. H. T. Brooke

Hughes Tool Company
Aircraft Division
Culver City, California
Attn: Mr. M. S. Harned

Hydronautics, Incorporated
Pindell School Road
Howard County
Laurel, Maryland
Attn: Mr. Phillip Eisenberg

Rand Development Corporation
13600 Deise Avenue
Cleveland 10, Ohio
Attn: Dr. A. S. Iberall

U. S. Rubber Company
Research and Development Department
Wayne, New Jersey
Attn: Mr. L. M. White

Technical Research Group, Inc.
2 Aerial Way
Syosset, Long Island, New York
Attn: Mr. Jack Kotik

Mr. C. Wigley
Flat 102
6-9 Charterhouse Square
London, E. C. 1, England

AVCO Corporation
Lycoming Division
1701 K Street, N. W.
Apt. No. 904
Washington, D. C.
Attn: Mr. T. A. Duncan

Mr. J. G. Baker
Baker Manufacturing Company
Evansville, Wisconsin

Curtiss-Wright Corporation Research Division
Turbomachinery Division
Quehanna, Pennsylvania
Attn: Mr. George H. Pedersen

Dr. Blaine R. Parkin
AiResearch Manufacturing Corporation
9851-9951 Sepulveda Boulevard
Los Angeles 45, California

The Boeing Company
Aero-Space Division
Seattle 24, Washington
Attn: Mr. R. E. Bateman
(Internal Mail Station 46-74)

Lockheed Aircraft Corporation
California Division
Hydrodynamics Research
Burbank, California
Attn: Mr. Bill East

National Research Council
Montreal Road
Ottawa 2, Canada
Attn: Mr. E. S. Turner

The Rand Corporation
1700 Main Street
Santa Monica, California
Attn: Technical Library

Stanford University
Department of Civil Engineering
Stanford, California
Attn: Dr. Byrne Perry
Dr. E. Y. Hsu

Dr. Hirsh Cohen
IBM Research Center
P. O. Box 218
Yorktown Heights, New York

Mr. David Wellinger
Hydrofoil Projects
Radio Corporation of America
Burlington, Massachusetts

Food Machinery Corporation
P. O. Box 367
San Jose, California
Attn: Mr. G. Tedrew

Dr. T. R. Goodman
Oceanics, Inc.
Technical Industrial Park
Plainview, Long Island, New York

Professor Brunelle
Department of Aeronautical Engineering
Princeton University
Princeton, New Jersey

Commanding Officer
Office of Naval Research Branch Office
86 East Randolph Street
Chicago 1, Illinois